TITLE:
Stability Analysis of the CIP Scheme and its Applications in Fundamental Study of the Diffused Optical Tomography(Dissertation_全文)

AUTHOR(S):
Tanaka, Daiki

CITATION:
Tanaka, Daiki. Stability Analysis of the CIP Scheme and its Applications in Fundamental Study of the Diffused Optical Tomography. 京都大学, 2014, 博士(情報学)

ISSUE DATE:
2014-03-24

URL:
https://doi.org/10.14989/doctor.k18416

RIGHT:

京都大学学術情報リポジトリ
KURENAI 紅
Kyoto University Research Information Repository

Stability Analysis of the CIP Scheme and its Applications in Fundamental Study of the Diffused Optical Tomography

TANAKA Daiki
Graduate School of Informatics, Kyoto University

Abstract

A stability estimate for the CIP scheme is shown. The scheme is intended to give accurate numerical solutions to linear hyperbolic partial differential equations of the first order, but the rigorous proof for its stability has been an open problem. We prove weak stability for the scheme. Furthermore, we apply it to numerical computation of the transport equation, which is a mathematical model for the diffused optical tomography.

Contents

1 Introduction

The diffused optical tomography (DOT) is considered as one of the ongoing medical tomographies. Since we use near-infrared light in DOT, we remark it to be a merit that human tissues are not exposed to radiation nor high magnetic field, and DOT is considered as a *non-invasive* tomography. It is well known that lights in biomedical tissues propagate with absorption and scattering, and we may consider light propagation as the migration of photons. Let $u(t, x, \xi)$ be the density of photons at time t and at position x with direction ξ, then a mathematical model of light propagation in biological tissues is considered as the following transport equation [1];

$$\frac{\partial}{\partial t}u(t,x,\xi) + \xi \cdot \nabla_x u(t,x,\xi) + \mu_t(x)u(t,x,\xi) = \mu_s(x)\int_{S^{d-1}} p(\xi,\xi')u(t,x,\xi')\, d\sigma_{\xi'}, \quad (1)$$

where S^{d-1} is the $(d-1)$-dimensional unit sphere and σ denotes the surface element along S^{d-1}. We regard DOT as an inverse problem to determine unknown coefficients $\mu_t(x)$ and $\mu_s(x)$ in the transport equation (1) from boundary measurement. Although near-infrared light is heavily scattered in biological tissue, it has been attempted to take out only the ballistic part from outgoing light by time-resolved measurement for small tissues such as brain of a mouse [6]. The author has tried to verify this approach by numerical computation. We discretized the 2-dimensional transport equation by the idea of the upwind scheme with the composite trapezoidal rule for an integral part in order to attempt numerical reconstruction of the coefficient $\mu_t(x)$. While, in the case without scattering, we could reconstruct μ_t by this method, in the case of highly-scattering media we should remark that reconstructed images were unclear and that reconstructed values were quite different from the exact ones. We are afraid that it is caused by low accuracy of the upwind scheme and we need to replace it to a high accurate scheme. We have adopted the CIP scheme for accurate computation, but we need to establish mathematical foundation to the scheme, and it is a background of the present research.

The CIP scheme is a finite difference scheme for the following first order partial differential equation, which is sometimes called an *advection equation*

$$\frac{\partial}{\partial t}u(t,x) + v\frac{\partial}{\partial x}u(t,x) = 0, \quad t > 0, x \in \mathbb{R},$$

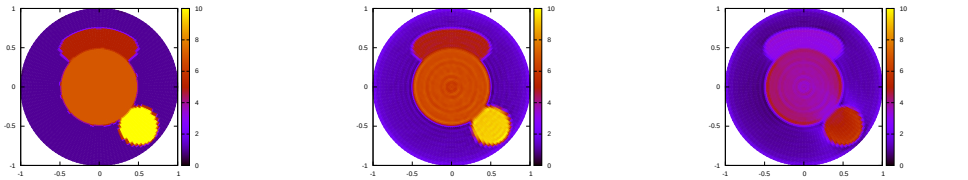

Exact μ_t | Reconstructed μ_t without scattering | Reconstructed μ_t in highly-scattering media

Figure 1: Numerical reconstruction of μ_t by the upwind scheme

where v is a real constant. The scheme was originally proposed by Takewaki, Nishiguchi and Yabe [25] in 1985. Various finite difference schemes have been proposed for this equation; for example, the upwind scheme [2] or the Lax-Wendroff scheme [11] etc.. Unlike the case of these conventional schemes, in the CIP scheme, we approximate not only u but also $\frac{\partial u}{\partial x}$, and this is the key idea for the CIP scheme. We remark, by this idea, the scheme attains high-accuracy. The name of the scheme "CIP" was originally abbreviation of *Cubic Interpolated Pseudo-particle* in [25], and it came to be called *Cubic Interpolated Propagation* [26] in 1993. In the original CIP scheme [25], values of functions between two adjacent grid points are interpolated by *cubic* polynomials, and this is the reason why its name is "Cubic Interpolated Propagation/Pseudo-particle". In 1996, however, Xiao, Yabe and Ito [27] proposed a variation of the CIP scheme, which is called RCIP scheme. Instead of cubic polynomials, rational functions are adopted to interpolate values of functions between adjacent grid points in the RCIP scheme. Yabe has proposed a new name to cover all the types of the schemes in [28], and "CIP" is considered as the abbreviation of the new name *Constrained Interpolation Profile*. Our analysis in this paper is based on the original CIP scheme.

The stability of a finite difference scheme means boundedness of exact solution of the scheme, and it is considered that the stability of a difference scheme guarantees its stable computation. For technical discussions, several definitions of the stability have been proposed. In 1956, Lax and Richtmyer [10] gave a definition of stability of finite difference schemes, which is called the *strong stability* [24] or simply *stability*. In 1960, Forsythe and Wasow [5] stated another definition of stability, which is called the *weak stability* [24][19]. Furthermore we find Kreiss' definition of stability [9], which is equivalent to that of Lax-Richtmyer for the case of constant coefficients. In 1968, Wendroff [24] discussed the weak and the strong stability in view of the amplification

matrix. In 1969, Thomée [19] stated both the weak and the strong stability in view of Sobolev spaces. In the following section, we prove the weak stability of the CIP scheme following the definition by Wendroff.

Under a suitable condition, the upwind scheme and the Lax-Wendroff scheme for a first order equation with constant coefficients are stable in the sense of Lax-Richtmyer. However, the stability of the CIP scheme has been an open problem. Only few attempts have so far been made at the stability analysis of the CIP scheme. Utsumi, Kunugi and Aoki estimated numerically the spectral radius of the amplification matrix [22], and Nara and Takaki [12] tried to prove the stability of the CIP scheme. However, their argument was incomplete from a view point of mathematics. We will give a complete proof for the stability of the CIP scheme in the present research.

This paper contains of four sections. In section 2, we prove the stability of the CIP scheme. Firstly, we will clarify conceptions of stability of finite difference methods. We will give the definition of both the weak stability and the strong stability. Secondly, we introduce the CIP scheme, and we prove that the CIP scheme is not strongly stable but weakly stable. This is the main mathematical result of the present paper. In section 3, we will show some numerical results by the CIP scheme. To begin with, we deal with a 1-dimensional first order hyperbolic equation with constant coefficient. We compare numerical results by the CIP scheme with those by the upwind and by the Lax-Wendroff scheme. We will also show numerical results of 2-dimensional first order hyperbolic equations with constant or variable coefficients. We should note that we give a mathmatical proof for the stability only for 1-dimensional cases, but we are optimistic for 2-dimensional cases though we do not give a rigorous proof here. This should be a future work. Finally, in section 4, we apply the CIP scheme to the 2-dimensional transport equation and discuss feasibility of DOT with time-resolved measurement, and we remark that it is the motivation of our analysis of the CIP scheme. We will introduce the Radon transform and show how to compute its inverse transform. We will compare numerical reconstruction of the attenuation coefficient by the CIP scheme with those by the upwind scheme, and we conclude our computation by the CIP scheme is fruitful in fundamental study of DOT.

2 Mathematical Analysis of the CIP Scheme

The purpose of this section is to prove that the CIP scheme is weakly stable. We firstly discuss various definitions of stability of finite difference schemes, and we show that the CIP scheme is not strongly but weakly stable.

2.1 Stability of Finite Difference Schemes

Let T be a positive number given in advance, let $\Delta t, \Delta x$ be positive numbers and let $S_{\Delta x}$ be a shift operator on $L^2(\mathbb{R})$ such that

$$(S_{\Delta x} f)(x) = f(x + \Delta x), \quad \text{for } f \in L^2(\mathbb{R}).$$

Let $\{U^n(x)\}_{0 \le n \le \lfloor \frac{T}{\Delta t} \rfloor}$ be a family of $\mathbb{R}^N$-valued functions of $x \in \mathbb{R}$. We consider the following finite difference scheme with constant coefficients, where $\lfloor t \rfloor$ denotes the largest integer less than or equal to t:

$$U^n(x) = \sum_{|j| \le q} Q_j(\Delta x, \Delta t) S_{\Delta x}^j U^{n-1}(x), \quad 1 \le n \le \left\lfloor \frac{T}{\Delta t} \right\rfloor, x \in \mathbb{R}, \tag{2}$$

$$U^0(x) \in L^2(\mathbb{R}), \tag{3}$$

where $Q_j(\Delta x, \Delta t)$ denotes a $(N \times N)$-matrix.

The stability in the sense of Forsythe-Wasow and in the sense of Lax-Richtmyer is defined as follows:

Definition 2.1. The finite difference scheme (2)–(3) is said to be *stable in the sense of Forsythe-Wasow* [5], if there exist a positive constant K and a non-negative number α such that

$$\|U^n\|_{L^2(\mathbb{R})} \le K \Delta t^{-\alpha} \left\|U^0\right\|_{L^2(\mathbb{R})}. \tag{4}$$

Especially in the case of $\alpha = 0$ in (4), the finite difference scheme (2)–(3) is said to be *stable in the sense of Lax-Richtmyer* [10],[17].

Applying the L^2-Fourier transform to the finite difference scheme (2)–(3), we obtain

$$\widehat{U}^{n+1}(\xi) = \sum_{|j| \le q} Q_j(\Delta x, \Delta t) \left(e^{i \Delta x \xi}\right)^j \widehat{U}^n(\xi), \quad 0 \le n \le \left\lfloor \frac{T}{\Delta t} \right\rfloor, \xi \in \mathbb{R}, \tag{5}$$

$$\widehat{U}^0(\xi) = \widehat{u}_0(\xi), \qquad \xi \in \mathbb{R}, \tag{6}$$

where $\widehat{U}^n(\xi)$ denotes the Fourier transform;

$$\widehat{U}^n(\xi) = \frac{1}{\sqrt{2\pi}} \int_{\mathbb{R}} e^{-ix\xi} U^n(x)\, dx.$$

The matrix $\widehat{Q}(e^{i\Delta x\xi}, \Delta x, \Delta t)$ defined by

$$\widehat{Q}(e^{i\Delta x\xi}, \Delta x, \Delta t) := \sum_{|j|\leq q} Q_j(\Delta x, \Delta t) \left(e^{i\Delta x\xi}\right)^j$$

is called the *amplification matrix*.

Wendroff [24] gives the definition of the weak and the strong stability as below.

Definition 2.2. The finite difference scheme (2)–(3) is said to be *weakly stable*, if there exist a positive constant K and a non-negative number s such that for $n = 0, 1, \ldots, \lfloor \frac{T}{\Delta t} \rfloor$,

$$\left| \widehat{Q}(e^{i\Delta x\xi}, \Delta x, \Delta t)^n \right| \leq K(1 + |\xi|^2)^{s/2}, \tag{7}$$

where $|\cdot|$ is a matrix norm. In the case of $s = 0$ in (7), the finite difference scheme (2)–(3) is said to be *strongly stable*.

Remark 2.1. Because all the norms are equivalent to one another in a finite dimensional space, the conception of both the weak and the strong stability does not depend upon a choice of matrix norm in (7).

We remark that the strong stability is equivalent to that in the sense of Lax-Richtmyer and that the weak stability is equivalent to that in the sense of Forsythe-Wasow [9].

To give estimates in Sobolev spaces for stable finite difference schemes, we introduce the usual Sobolev space by

$$H^s(\mathbb{R}) := \left\{ f(x) \in L^2(\mathbb{R}) \;\middle|\; \int_{\mathbb{R}} (1 + |\xi|^2)^s \left| \widehat{f}(\xi) \right|^2 d\xi < \infty \right\},$$
$$\|f\|_{H^s} := \left(\int_{\mathbb{R}} (1 + |\xi|^2)^s \left| \widehat{f}(\xi) \right|^2 d\xi \right)^{1/2},$$

where $s \geq 0$. Then we have the following proposition.

Proposition 2.1. *The finite difference scheme* (2)–(3) *is weakly stable if and only if there exist a positive constant K and a non-negative number s such that for all $U^0 \in H^s(\mathbb{R})$, $n = 0, 1, \ldots, \lfloor \frac{T}{\Delta t} \rfloor$,*

$$\left\| U^n \right\|_{L^2(\mathbb{R})} \leq K \left\| U^0 \right\|_{H^s(\mathbb{R})} \tag{8}$$

holds. The finite difference scheme (2)–(3) *is strongly stable if and only if* $s = 0$ *in* (8).

2.2 Stability Analysis of the CIP Scheme

We introduce the CIP scheme and state difference between the CIP scheme and the upwind or the Lax-Wendroff scheme. The aim of this subsection is to prove that the CIP scheme is not strongly stable but weakly stable.

Let T be a positive number given in advance and let $u(t, x)$ be a real valued function. Let us consider the following intial value problem for a 1-dimensional advection equation:

$$\frac{\partial}{\partial t}u(t,x) + v\frac{\partial}{\partial x}u(t,x) = 0, \qquad 0 < t < T, x \in \mathbb{R}, \tag{9}$$

$$u(0,x) = u_0(x), \quad x \in \mathbb{R}, \tag{10}$$

where v is a negative constant. For a smooth function $u_0 \in L^2(\mathbb{R})$, the exact solution to (9)–(10) is given by

$$u(t,x) = u_0(x - vt).$$

In particular, for an arbitrary positive number τ, the solution u satisfies

$$u(t+\tau, x) = u(t, x - v\tau). \tag{11}$$

To begin with, let us consider conventional finite difference schemes to (9)–(10); the upwind scheme and the Lax-Wendroff scheme. Let Δt and Δx be positive numbers, and let

$$\lambda := \frac{|v|\,\Delta t}{\Delta x}.$$

Assume $\lambda \leq 1$, then we have $x - v\Delta t \in [x, x + \Delta x]$. Let $U^n(x)$ be approximation of $u(n\Delta t, x)$. The upwind scheme to (9)–(10) is given by

$$U^{n+1}(x) = (1-\lambda)U^n(x) + \lambda U^n(x + \Delta x), \quad 0 \leq n \leq \left\lfloor \frac{T}{\Delta t} \right\rfloor - 1, x \in \mathbb{R},$$

$$U^0(x) = u_0(x), \qquad x \in \mathbb{R}.$$

In the upwind scheme, we may consider it as the simplest approximation along the x-axis; it implies the linear interpolation of the values of adjacent

two nodes. On the other hand, in the Lax-Wendroff scheme, we interpolate those by the *quadratic* polynomial $F_2(X)$ satisfying

$$F_2(x-\Delta x) = U^n(x-\Delta x), \quad F_2(x) = U^n(x), \quad F_2(x+\Delta x) = U^n(x+\Delta x);$$

that is

$$F_2(X) = \frac{U^n(x+\Delta x) - 2U^n(x) + U^n(x-\Delta x)}{2\Delta x^2}(X-x)^2 + \frac{U^n(x+\Delta x) - U^n(x-\Delta x)}{2\Delta x}(X-x) + U^n(x).$$

This leads us to the Lax-Wendroff scheme

$$U^{n+1}(x) = -\frac{1}{2}\lambda(1-\lambda)U^n(x-\Delta x) + (1-\lambda^2)U^n(x) + \frac{1}{2}\lambda(1+\lambda)U^n(x+\Delta x), \quad 0 \le n \le \left\lfloor \frac{T}{\Delta t} \right\rfloor - 1, x \in \mathbb{R},$$
$$U^0(x) = u_0(x), \quad x \in \mathbb{R}.$$

In the CIP scheme, we use *cubic* polynomials in interpolation.

Let us introduce the CIP scheme. We here compute not only u but also $\frac{\partial u}{\partial x}$, that is, we consider the following initial-value problem of a system of advection equations:

$$\frac{\partial}{\partial t}\begin{pmatrix} u(t,x) \\ \frac{\partial u}{\partial x}(t,x) \end{pmatrix} + v\frac{\partial}{\partial x}\begin{pmatrix} u(t,x) \\ \frac{\partial u}{\partial x}(t,x) \end{pmatrix} = 0, \qquad 0 < t \le T, x \in \mathbb{R},$$
$$\begin{pmatrix} u(0,x) \\ \frac{\partial u}{\partial x}(0,x) \end{pmatrix} = \begin{pmatrix} u_0(x) \\ \frac{du_0}{dx}(x) \end{pmatrix}, \qquad x \in \mathbb{R}.$$

Let us denote approximation of $\frac{\partial u}{\partial x}(n\Delta t, x)$ by $\partial U^n(x)$. Let $F_3(X)$ be a *cubic* polynomial satisfying

$$F_3(x) = U^n(x), \quad F_3(x+\Delta x) = U^n(x+\Delta x),$$
$$F_3'(x) = \partial U^n(x), \quad F_3'(x+\Delta x) = \partial U^n(x+\Delta x),$$

and it leads us to

$$F_3(X) = p^n(x)(X-x)^3 + q^n(x)(X-x)^2 + \partial U^n(x)(X-x) + U^n(x),$$

where

$$p^n(x) = \frac{\partial U^n(x) + \partial U^n(x+\Delta x)}{\Delta x^2} + 2\frac{U^n(x) - U^n(x+\Delta x)}{\Delta x^3}, \tag{12}$$

$$q^n(x) = -\frac{2\partial U^n(x) + \partial U^n(x+\Delta x)}{\Delta x} + 3\frac{U^n(x+\Delta x) - U^n(x)}{\Delta x^2}. \tag{13}$$

Using the polynomial $F_3(X)$, we set

$$U^{n+1}(x) = F_3(x - v\Delta t), \quad \partial U^{n+1}(x) = F_3'(x - v\Delta t). \tag{14}$$

Substituting (12)–(13) into (14), we obtain

$$\begin{aligned} U^{n+1}(x) &= (\lambda-1)^2(2\lambda+1)U^n(x) - \lambda^2(2\lambda-3)U^n(x+\Delta x) \\ &\quad + \lambda(\lambda-1)^2\Delta x\partial U^n(x) + \lambda^2(\lambda-1)\Delta x\partial U^n(x+\Delta x), \end{aligned} \tag{15}$$

$$\begin{aligned} \partial U^{n+1}(x) &= \frac{6\lambda(\lambda-1)}{\Delta x}(U^n(x) - U^n(x+\Delta x)) \\ &\quad + (\lambda-1)(3\lambda-1)\partial U^n(x) + \lambda(3\lambda-2)\partial U^{n+1}(x+\Delta x), \end{aligned} \tag{16}$$

$$U^0(x) = u_0(x), \quad \partial U^0(x) = \frac{du_0}{dx}(x). \tag{17}$$

This is the CIP scheme for (9)–(10).

Let us start stability analysis of the CIP scheme. By applying the Fourier transform to (15)–(17), we obtain

$$\begin{aligned} \widehat{U}^{n+1}(\xi) &= e^{i\psi}\left(a(r,\psi)\widehat{U}^n(\xi) + \Delta x\ b(r,\psi)\widehat{\partial U}^n(\xi)\right), \\ \widehat{\partial U}^{n+1}(\xi) &= e^{i\psi}\left(\frac{c(r,\psi)}{\Delta x}\widehat{U}^n(\xi) + d(r,\psi)\widehat{\partial U}^n(\xi)\right), \end{aligned}$$

where

$$\begin{aligned} a(r,\psi) &= \cos\psi + ir(-4r^2+3)\sin\psi, \\ b(r,\psi) &= \frac{4r^2-1}{4}(2r\cos\psi + i\sin\psi), \\ c(r,\psi) &= -3(4r^2-1)i\sin\psi, \\ d(r,\psi) &= \frac{1}{2}(12r^2-1)\cos\psi + i2r\sin\psi, \\ \psi &= \frac{\xi\Delta x}{2}, \quad r = \lambda - \frac{1}{2}. \end{aligned}$$

Hence we show that the CIP scheme is *not* strongly stable. We should remark

that λ must satisfy $\lambda \leq 1$.

Theorem 2.1. *When $\lambda < 1$, the CIP scheme (15)–(17) is not strongly stable.*

Proof. Let $\widehat{Q}(r,\psi)$ be the amplification matrix, then we have

$$\left|\widehat{Q}(r,\psi)\right| = \left|e^{i\psi}\begin{pmatrix} a & \Delta x b \\ \frac{c}{\Delta x} & d \end{pmatrix}\right| \geq 3(1-4r^2)\left|\frac{\sin\psi}{\Delta x}\right|, \tag{18}$$

where $|Q|$ denotes the entrywise 1-norm of Q, that is

$$\left|\widehat{Q}(r,\psi)\right| := |a| + |\Delta x b| + \left|\frac{c}{\Delta x}\right| + |d|\,.$$

Because the right hand side of (18) is not uniformly bounded when $\Delta x \to 0$, the CIP scheme is not strongly stable. □

Remark 2.2. $\lambda = 1$ is the exceptional case, and we have

$$U^n(x) = u_0(x - nv\Delta t), \quad \partial U^n(x) = \frac{du_0}{dx}(x - nv\Delta t).$$

We note that the numerical solution by the CIP scheme coincides with the exact one.

To prove the weak stability of the CIP scheme, we need to estimate eigenvalues of the amplification matrix $\widehat{Q}(r,\psi)$. Let σ_+ and σ_- be the eigenvalues of $\widehat{Q}(r,\psi)$, then we have

$$\sigma_\pm = \alpha(r,\psi) + i\beta(r,\psi) \pm \frac{1-4r^2}{2}\sqrt{\gamma(r,\psi) + i\delta(r,\psi)},$$

where

$$\alpha(r,\psi) = \frac{12r^2+1}{4}\cos\psi, \qquad \beta(r,\psi) = \frac{r(-4r^2+5)}{2}\sin\psi,$$
$$\gamma(r,\psi) = \frac{9}{4}\cos^2\psi + (3-r^2)\sin^2\psi, \quad \delta(r,\psi) = -3r\sin\psi\cos\psi.$$

We have the following lemma.

Lemma 2.1. (Nara and Takaki [12])
If $\lambda \leq 1$, then an eigenvalue σ of $\widehat{Q}(r,\psi)$ satisfies $|\sigma| \leq 1$.

Proof. This proof is due to Nara and Takaki [12]. In the case that $r = \pm\frac{1}{2}$ or $\cos\psi = \pm 1$, the result is trivial. We assume that $r \in (-\frac{1}{2}, \frac{1}{2})$ and $\cos\psi \in (-1, 1)$. Then $|\sigma|^2 = 1$ gives

$$\frac{(1-4r^2)^4}{256}(\cos^2\psi - 1)^2\left[\left\{(1-4r^2)^2\cos^2\psi - (16r^4+7)\right\}^2 + 128r^2(4r^2+3)\right] = 0.$$

It follows from what has been said that the signature of $|\sigma| - 1$ is invariant in the domain $\{(r,\psi) \mid r \in (-\frac{1}{2}, \frac{1}{2}), \psi \in (0,\pi)\}$. When $(r,\psi) = (0, \frac{\pi}{2})$, we have $|\sigma| = \frac{\sqrt{3}}{2} < 1$. Therefore $|\sigma| < 1$ in the domain $\{(r,\psi) \mid r \in (-\frac{1}{2}, \frac{1}{2}), \psi \in (0,\pi)\}$. □

Let us define complex-valued functions $a_n(r,\psi), b_n(r,\psi), c_n(r,\psi)$ and $d_n(r,\psi)$ as entries of $\widehat{Q}(r,\psi)^n$;

$$\widehat{Q}(r,\psi)^n = e^{in\psi}\begin{pmatrix} a_n(r,\psi) & \Delta x b_n(r,\psi) \\ \frac{c_n(r,\psi)}{\Delta x} & d_n(r,\psi) \end{pmatrix}.$$

Then we have the following estimates.

Proposition 2.2. *If $\lambda \leq 1$, then there exists a positive constant K such that*

$$|a_n|, |b_n|, |d_n|, \left|\frac{c_n}{\sin\psi}\right| \leq K.$$

Proof. Let σ_+, σ_- be the eigenvalues of $\widehat{Q}$ and let

$$P = \begin{pmatrix} \sigma_+ - d & \sigma_- - d \\ c & c \end{pmatrix}.$$

Then we have

$$P^{-1}\widehat{Q}P = \begin{pmatrix} \sigma_+ & 0 \\ 0 & \sigma_- \end{pmatrix}.$$

Hence we have

$$\begin{aligned}\widehat{Q}^n &= P(P^{-1}\widehat{Q}P)^n P^{-1} \\ &= \frac{1}{c(\sigma_+ - \sigma_-)}\begin{pmatrix} c(\sigma_+^n(\sigma_+ - d) - \sigma_-^n(\sigma_- - d)) & (\sigma_+^n - \sigma_-^n)(\sigma_+ - d)(\sigma_- - d) \\ c^2(\sigma_+^n - \sigma_-^n) & c(\sigma_-^n(\sigma_+ - d) - \sigma_+^n(\sigma_- - d)) \end{pmatrix}.\end{aligned}$$

Firstly, we prove that $a_n(r,\psi)$ and $d_n(r,\psi)$ are bounded. Because of

$r \in (-\frac{1}{2}, \frac{1}{2}]$, we have $|\gamma(r,\psi)| \geq \frac{9}{4}$, and we obtain

$$\left|\sqrt{\gamma + i\delta}\right| \geq \left|\mathrm{Re}\left(\sqrt{\gamma + i\delta}\right)\right| \geq \frac{3}{2}.$$

We note $\gamma + i\delta = (\frac{3}{2}\cos\psi - ri\sin\psi)^2 + 3\sin^2\psi$, and we have

$$\left|\sqrt{\gamma + i\delta}\right| \leq \left|\frac{3}{2}\cos\psi - ri\sin\psi\right| + \sqrt{3}\left|\sin\psi\right|.$$

Hence we have

$$\begin{aligned}
|a_n| &= \left|\frac{c(\sigma_+^n(\sigma_+ - d) - \sigma_-^n(\sigma_- - d))}{c(\sigma_+ - \sigma_-)}\right| \\
&\leq \frac{2}{3}\left(\frac{3}{2}\left|\cos\psi\right| + \left|r\sin\psi\right| + \left|\sqrt{\gamma + i\delta}\right|\right),
\end{aligned}$$

$$\begin{aligned}
|d_n| &= \left|\frac{c(\sigma_-^n(\sigma_+ - d) - \sigma_+^n(\sigma_- - d))}{c(\sigma_+ - \sigma_-)}\right| \\
&\leq \frac{2}{3}\left(\frac{3}{2}\left|\cos\psi\right| + \left|r\sin\psi\right| + \left|\sqrt{\gamma + i\delta}\right|\right),
\end{aligned}$$

and they imply that $a_n(r,\psi)$ and $d_n(r,\psi)$ are bounded.

Secondly, we prove that $b_n(r,\psi)$ is bounded. Since σ_+ is an eigenvalue of $\widehat{Q}$ and $(\sigma_+ - d, c)^T$ is an eigenvector corresponding to σ_+, we have

$$\begin{aligned}
(\sigma_+ - d)(\sigma_- - d) &= -\frac{bc}{a - \sigma_+}(\sigma_- - d) \\
&= -\frac{bc}{(1 - 4r^2)\left(\frac{3}{4}\cos\psi + \frac{r}{2}i\sin\psi - \frac{1}{2}\sqrt{\gamma + i\delta}\right)}(\sigma_- - d) \\
&= -\frac{bc}{(\sigma_- - d)}(\sigma_- - d) \\
&= -bc.
\end{aligned}$$

Then we have

$$|b_n| = \left|\frac{(\sigma_+^n - \sigma_-^n)(\sigma_+ - d)(\sigma_- - d)}{c(\sigma_+ - \sigma_-)}\right|$$

$$= \left| \frac{(\sigma_+^n - \sigma_-^n)(-bc)}{c(\sigma_+ - \sigma_-)} \right|$$
$$\leq \frac{1}{3}(2\,|r\cos\psi| + |\sin\psi|).$$

Hence we have $b_n(r,\psi)$ is bounded.

Finally, we prove that $\frac{c_n}{\sin\psi}$ is bounded;

$$\left| \frac{c_n}{\sin\psi} \right| = \left| \frac{c^2(\sigma_+^n - \sigma_-^n)}{\sin\psi c(\sigma_+ - \sigma_-)} \right|$$
$$= \left| \frac{3(1-4r^2)\sin\psi(\sigma_+^n - \sigma_-^n)}{\sin\psi(1-4r^2)\sqrt{\gamma + i\delta}} \right| \leq 4.$$

This completes our proof. □

Using the proposition above, we can prove our main theorem.

Theorem 2.2. (Weak stability of the CIP scheme)
If $\lambda \leq 1$, then the CIP scheme (15)–(17) is weakly stable.

Proof. For the amplification matrix $\widehat{Q}(r,\psi)$ of the CIP scheme (15)–(17), using Proposition 2.2, we have

$$\left| \widehat{Q}(r,\psi)^n \right| = |a_n(r,\psi)| + |\Delta x b_n(r,\psi)| + \left| \frac{c_n(r,\psi)}{\Delta x} \right| + |d_n(r,\psi)|$$
$$\leq K + \Delta x K + \left| \frac{c_n(r,\psi)}{\sin\psi} \frac{\sin\psi}{\psi} \frac{\xi}{2} \right| + K$$
$$\leq (2 + \Delta x)K + \frac{K}{2}\,|\xi| \leq K'(1 + |\xi|^2)^{1/2},$$

where K' is a positive constant. This completes our proof. □

Using Proposition 2.2, we obtain the following a priori estimate for the CIP scheme.

Theorem 2.3. *Let $U^n(x)$ and $\partial U^n(x)$ be the solution to the CIP scheme (15)–(17). If $\lambda \leq 1$, then there exists a positive number K such that for $u_0(x) \in H^1(\mathbb{R})$*

$$\|U^n\|_{L^2} \leq (1 + \Delta x)K \|u_0\|_{H^1}, \tag{19}$$

$$\|\partial U^n\|_{L^2} \leq \frac{3K}{2} \|u_0\|_{H^1}. \tag{20}$$

Proof. The inequality (19) follows immediately from Proposition 2.2. Let us prove (20). Because $i\xi\widehat{U}^0(\xi) = \widehat{\partial U}^0(\xi)$, we have

$$\begin{aligned}
\left|\widehat{\partial U}^n\right| &\leq \left|\frac{c_n}{\Delta x}\widehat{U}^0\right| + \left|d_n\widehat{\partial U}^0\right| \\
&= \left|\frac{1}{2}\cdot\frac{c_n}{\sin\psi}\cdot\frac{\sin\psi}{\psi}\cdot i\xi\widehat{U}^0\right| + \left|d_n\widehat{\partial U}^0\right| \\
&\leq \frac{3K}{2}\left|\widehat{\partial U}^0\right|.
\end{aligned}$$

Then (20) follows from the Plancherel theorem. □

Finally, we will prove that the solution to the CIP scheme converges to the exact solution as $\Delta t \to 0$.

Theorem 2.4. (Convergency of the CIP scheme)
Let $\lambda \in (0,1]$ and $t \in (0,T)$ be fixed. Suppose $u_0 \in H^1(\mathbb{R})$ and assume Δx satisfies $\Delta x = \frac{|v|\Delta t}{\lambda}$. Let $U^n(x)$ and $\partial U^n(x)$ be the solution to the CIP scheme (15)–(17) and let $u(t,x)$ be the exact solution to the (9)–(10). Then we have

$$\lim_{\Delta t\to+0}\left\|U^N - u(t,\cdot)\right\|_{L^2(\mathbb{R})} = 0, \quad \lim_{\Delta t\to+0}\left\|\partial U^N - \frac{\partial u}{\partial x}(t,\cdot)\right\|_{L^2(\mathbb{R})} = 0,$$

where $N = \left\lfloor \frac{t}{\Delta t}\right\rfloor$.

Proof. In the case $\lambda = 1$, the result is trivial. We assume $0 < \lambda < 1$. Because $C_0^\infty(\mathbb{R})$ is dense in $H^1(\mathbb{R})$, it is enough to show the case of $u_0 \in C_0^\infty(\mathbb{R})$. At this time, we have $u(t,x) = u_0(x-t)$. Because of the weak stability of the CIP scheme (15)–(17), there exists a positive number K such that

$$\left|\widehat{Q}(r,\psi)^N\right| \leq K(1+\left|\xi^2\right|)^{1/2}.$$

Let ε be a positive number. Then using the Plancherel theorem, for sufficiently large R

$$\left\|\begin{pmatrix} U^N \\ \partial U^N\end{pmatrix} - \begin{pmatrix} u(t) \\ \frac{\partial u}{\partial x}(t)\end{pmatrix}\right\|_{L^2(\mathbb{R})} = \left\|\begin{pmatrix} \widehat{U}^N \\ \widehat{\partial U}^N\end{pmatrix} - \begin{pmatrix} \widehat{u}(t) \\ \widehat{\frac{\partial u}{\partial x}}(t)\end{pmatrix}\right\|_{L^2(\mathbb{R})}$$

$$
\begin{aligned}
&= \left(\int_{\mathbb{R}} \left| \left(\widehat{Q}(r,\psi)^N - e^{-ivt\xi} I \right) \begin{pmatrix} \widehat{u}_0(\xi) \\ i\xi \widehat{u}_0(\xi) \end{pmatrix} \right|^2 \, d\xi \right)^{1/2} \\
&\leq \left(\int_{|\xi|<R} \left| \left(\widehat{Q}(r,\psi)^N - e^{-ivt\xi} I \right) \begin{pmatrix} \widehat{u}_0(\xi) \\ i\xi \widehat{u}_0(\xi) \end{pmatrix} \right|^2 \, d\xi \right)^{1/2} \\
&\qquad + (K+1) \left(\int_{|\xi|\geq R} (1+|\xi|^2) \left| \widehat{u}_0(\xi) \right|^2 \, d\xi \right)^{1/2} \\
&\leq \left(\int_{|\xi|<R} \left| \left(\widehat{Q}(r,\psi)^N - e^{-ivt\xi} I \right) \begin{pmatrix} \widehat{u}_0(\xi) \\ i\xi \widehat{u}_0(\xi) \end{pmatrix} \right|^2 \, d\xi \right)^{1/2} + \varepsilon.
\end{aligned}
$$

Then we have

$$
\begin{aligned}
&\left(\int_{|\xi|<R} \left| \left(\widehat{Q}(r,\psi)^N - e^{-ivt\xi} I \right) \begin{pmatrix} \widehat{u}_0(\xi) \\ i\xi \widehat{u}_0(\xi) \end{pmatrix} \right|^2 \, d\xi \right)^{1/2} \\
&\qquad \leq \left(\int_{|\xi|<R} \left| \left(\widehat{Q}(r,\psi)^N - e^{-ivN\Delta t\xi} I \right) \begin{pmatrix} \widehat{u}_0(\xi) \\ i\xi \widehat{u}_0(\xi) \end{pmatrix} \right|^2 \, d\xi \right)^{1/2} \\
&\qquad\qquad + \left(\int_{|\xi|<R} \left| \left(e^{-ivN\Delta t\xi} I - e^{-ivt\xi} I \right) \begin{pmatrix} \widehat{u}_0(\xi) \\ i\xi \widehat{u}_0(\xi) \end{pmatrix} \right|^2 \, d\xi \right)^{1/2}.
\end{aligned}
$$

By Lebesgue's dominated convergence theorem, for sufficiently small Δt, we have

$$
\left(\int_{|\xi|<R} \left| \left(e^{-ivN\Delta t\xi} I - e^{-ivt\xi} I \right) \begin{pmatrix} \widehat{u}_0(\xi) \\ i\xi \widehat{u}_0(\xi) \end{pmatrix} \right|^2 \, d\xi \right)^{1/2} < \varepsilon.
$$

Using Taylor's theorem, we obtain

$$
\begin{aligned}
&\begin{pmatrix} U^1(x) \\ \partial U^1(x) \end{pmatrix} - \begin{pmatrix} u(\Delta t, x) \\ \frac{\partial u}{\partial x}(\Delta t, x) \end{pmatrix} = \\
&\begin{pmatrix} \int_0^{\Delta x} u_0^{(4)}(x+s) \left\{ (-v\Delta t)^3 \left(\frac{(\Delta x - s)^2}{2\Delta x^2} + \frac{(\Delta x - s)^3}{3\Delta x^3} \right) + (-v\Delta t)^2 \left(\frac{(\Delta x - s)^2}{2\Delta x} + \frac{(\Delta x - s)^3}{2\Delta x^2} \right) \right\} \, ds \\ \int_0^{\Delta x} u_0^{(4)}(x+s) \left\{ 3(-v\Delta t)^2 \left(\frac{(\Delta x - s)^2}{2\Delta x^2} + \frac{(\Delta x - s)^3}{3\Delta x^3} \right) + 2(-v\Delta t) \left(\frac{(\Delta x - s)^2}{2\Delta x} + \frac{(\Delta x - s)^3}{2\Delta x^2} \right) \right\} \, ds \end{pmatrix} \\
&\qquad\qquad - \begin{pmatrix} \int_0^{-v\Delta t} u_0^{(4)}(x+s) \frac{(-v\Delta t - s)^3}{6} \, ds \\ \int_0^{-v\Delta t} u_0^{(4)}(x+s) \frac{(-v\Delta t - s)^2}{2} \, ds \end{pmatrix},
\end{aligned}
$$

and we have

$$
\begin{aligned}
&\int_{|\xi|<R} \left| \left(\widehat{Q}(r,\psi)^N - e^{-ivN\Delta t\xi} I \right) \begin{pmatrix} \widehat{u}_0(\xi) \\ i\xi \widehat{u}_0(\xi) \end{pmatrix} \right|^2 \, d\xi \\
&\quad \leq \int_{|\xi|<R} \left| \widehat{Q}(r,\psi)^{N-1} + e^{-iv\Delta t\xi} \widehat{Q}(r,\psi)^{N-2} + \cdots + e^{-ivN\Delta t\xi} I \right|^2 \\
&\qquad\qquad \times \left| \left(\widehat{Q}(r,\psi) - e^{-iv\Delta t\xi} I \right) \begin{pmatrix} \widehat{u}_0(\xi) \\ i\xi \widehat{u}_0(\xi) \end{pmatrix} \right|^2 \, d\xi \\
&\quad \leq K^2 N^2 \int_{|\xi|<R} (1+|\xi|^2) \\
&\qquad\qquad \times \left| (i\xi)^4 \widehat{u}_0(\xi) \begin{pmatrix} \frac{5}{6} |v\Delta t|^3 \Delta x + |v\Delta t|^2 \Delta x^2 + \frac{1}{6} |v\Delta t|^4 \\ \frac{5}{2} |v\Delta t|^2 \Delta x + 2 |v\Delta t| \Delta x^2 + \frac{1}{2} |v\Delta t|^3 \end{pmatrix} \right|^2 \, d\xi \\
&\quad \leq \frac{Ct^2}{\Delta t^2} \left| \begin{pmatrix} \Delta t^4 \\ \Delta t^3 \end{pmatrix} \right|^2 \|u_0\|^2_{L^2(\mathbb{R})} ,
\end{aligned}
$$

where C is a positive number. Then we have, for sufficiently small Δt

$$
\left\| \begin{pmatrix} U^N \\ \partial U^N \end{pmatrix} - \begin{pmatrix} u(t) \\ \frac{\partial u}{\partial x}(t) \end{pmatrix} \right\|_{L^2(\mathbb{R})} \leq Ct \left| \begin{pmatrix} \Delta t^3 \\ \Delta t^2 \end{pmatrix} \right| \|u_0\|_{L^2(\mathbb{R})} + 2\varepsilon < 3\varepsilon.
$$

This completes the proof. □

3 Some Applications of the CIP Scheme

In this section, we show numerical results by the CIP scheme. We firstly consider the initial value problem for a 1-dimensional advection equation with a constant coefficient. We compare numerical results by the CIP scheme with those by the upwind scheme and by the Lax-Wendroff scheme. We also consider the initial value problem for a 2-dimensional advection equation with constant coefficients. We firstly introduce a 2-dimensional CIP scheme, which we do not mention in the previous section, and show some numerical results by the scheme. Lastly, we apply the CIP scheme to the initial value problem for a 2-dimensional advection equation with variable coefficients.

3.1 1-dimensional Advection Equation with a Constant Coefficient

We show some numerical results of a 1-dimensional advection equation on the 1-dimensional torus $\mathbb{T}^1 = [0,1]/\sim$, where we identify 0 and 1 by an equivalence relation $\sim$. We compute the 1-dimensional advection equation by three schemes; the first one is the upwind scheme, the second is the Lax-Wendroff scheme and the last is the CIP scheme.

Let us consider the intial value problem of the following 1-dimensional advection equation;

$$\frac{\partial u}{\partial t}(t,x) + \frac{\partial u}{\partial x}(t,x) = 0, \quad t > 0, x \in \mathbb{T}^1, \tag{21}$$

$$u(0,x) = u_0(x), \quad x \in \mathbb{T}^1. \tag{22}$$

We take three functions $u_1(x), u_2(x), u_3(x)$ as the initial function $u(0,x)$: the first one is a rectangle pulse function;

$$u_1(x) = \begin{cases} 1 & \frac{1}{4} < x < \frac{1}{2} \\ 0 & \text{otherwise,} \end{cases}$$

the second is a triangle pulse function;

$$u_2(x) = \begin{cases} 8x - 2 & \frac{1}{4} < x \leq \frac{3}{8} \\ -8x + 4 & \frac{3}{8} < x < \frac{1}{2} \\ 0 & \text{otherwise,} \end{cases}$$

and the last is a sine function;

$$u_3(x) = \sin 2\pi x.$$

For discretization of the initial value problem (21)–(22), let $\Delta t, \Delta x$ be positive numbers and let $\lambda := \frac{\Delta t}{\Delta x}$. Let $U^n(x)$ be approximation of $u(n\Delta t, x)$ and let $\partial U^n(x)$ be that of $\frac{\partial u}{\partial x}(n\Delta t, x)$. We note that the coefficient of $\frac{\partial u}{\partial x}$ is positive and the schemes need suitable change from those in the previous section. The upwind scheme is given by

$$U^{n+1}(x) = (1-\lambda)U^n(x) + \lambda U^n(x - \Delta x),$$

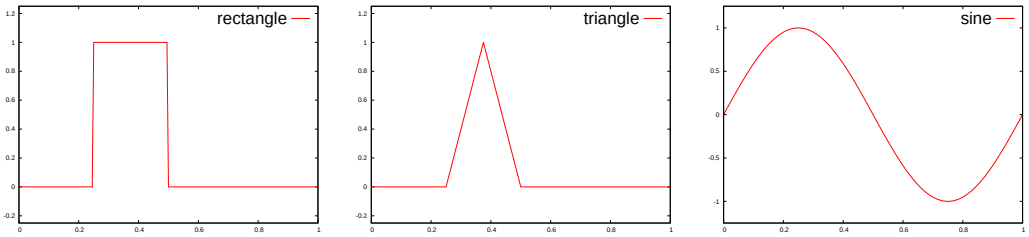

Rectangle pulse $u_1(x)$ Triangle pulse $u_2(x)$ Sine $u_3(x)$

Figure 2: Initial functions of (22)

the Lax-Wendroff scheme is given by

$$U^{n+1}(x) = \frac{1}{2}\lambda(1+\lambda)U^n(x-\Delta x) + (1-\lambda^2)U^n(x) - \frac{1}{2}\lambda(1-\lambda)U^n(x+\Delta x),$$

and the CIP scheme is given by

$$\begin{aligned} U^{n+1}(x) &= (\lambda+1)^2(-2\lambda+1)U^n(x) + \lambda^2(2\lambda+1)U^n(x-\Delta x) \\ &\quad - \Delta x\lambda(\lambda-1)^2\partial U^n(x) - \Delta x\lambda(\lambda-1)\partial U^n(x-\Delta x), \\ \partial U^{n+1}(x) &= \frac{6}{\Delta x}\lambda(1-\lambda)(U^n(x) - U^n(x-\Delta x)) \\ &\quad + (\lambda-1)(3\lambda-1)\partial U^n(x) + \lambda(3\lambda-2)\partial U^n(x-\Delta x). \end{aligned}$$

Figure 3, Figure 4 and Figure 5 show their numerical results. In these figures, red lines stand for numerical solutions and blue lines stand for the exact ones. In these results, the discretization parameters are $\Delta t = 1/400$, $\Delta x = 1/200$ and $\lambda = 1/2$. Figure 3 shows numerical results for the case $u(0,x) = u_1(x)$, Figure 4 shows numerical results for the case $u(0,x) = u_2(x)$, and Figure 5 shows numerical results for the case $u(0,x) = u_3(x)$. In all the cases, the numerical solutions by the upwind scheme rapidly converge to constant functions and the graph profiles of the initial functions are completely lost. Numerical solutions by the Lax-Wendroff scheme oscillate after the singularity (discontinuity) in Figure 3 and Figure 4. This is a well-known feature of the Lax-Wendroff scheme. In Figure 5, numerical solution by the Lax-Wendroff scheme shows decay and gradual delay. After a long time, numerical results by the Lax-Wendroff scheme becomes quite different from the exact solution in each case. On the other hand, numerical solutions by the CIP scheme seem to be quite accurate. For the rectangle pulse, a solution by the CIP scheme has small overshoot before and after its discontinuities, but we should remark that the overshoot does not growth with time going.

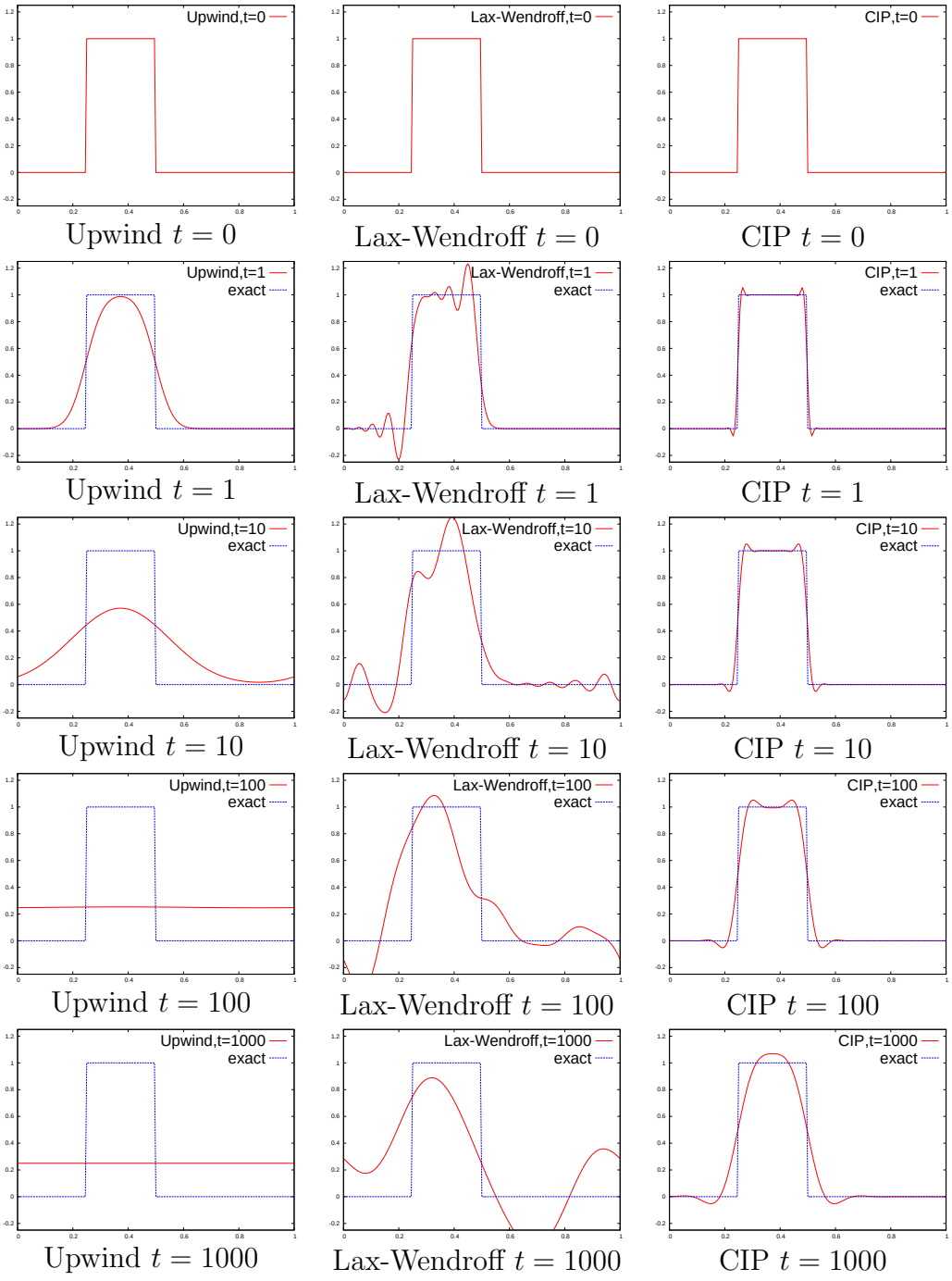

Figure 3: Numerical results for rectangle pulse $u_1(x)$

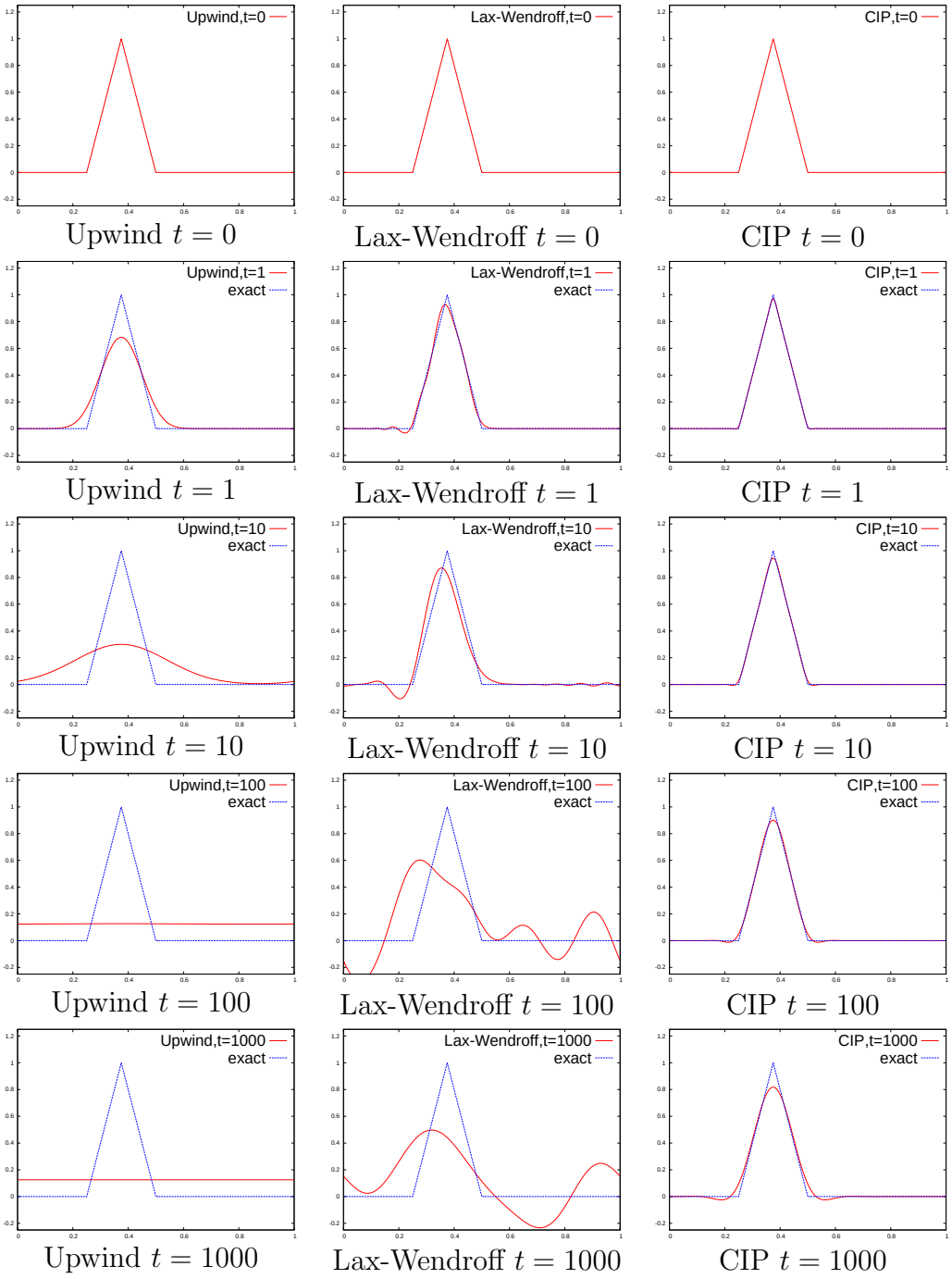

Figure 4: Numerical results for triangle pulse $u_2(x)$

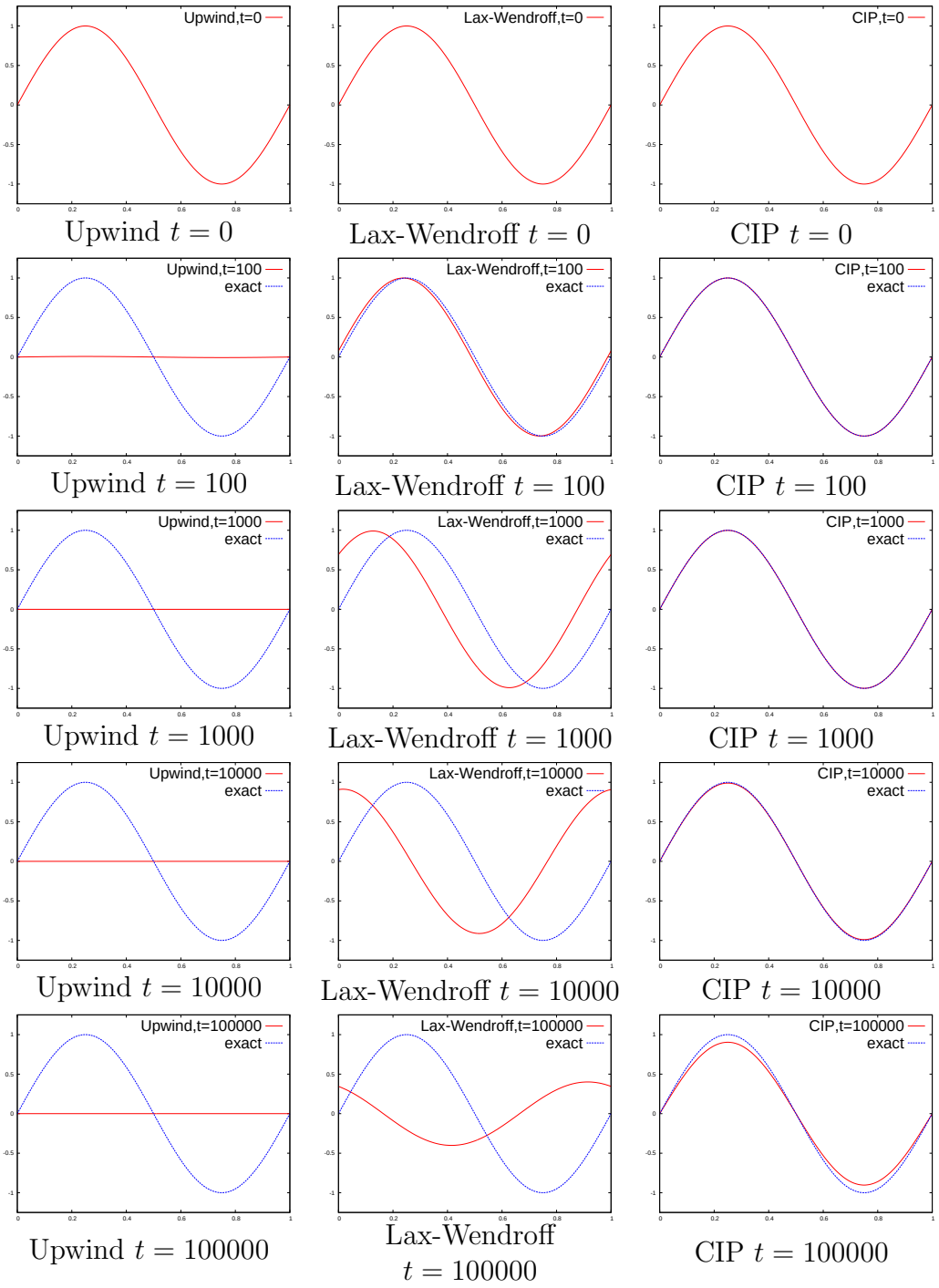

Figure 5: Numerical results for sine curve $u_3(x)$

3.2 2-dimensional Advection Equation with Variable Coefficients

We here show numerical results of a 2-dimensional CIP scheme. We firstly introduce a 2-dimensional CIP scheme to show numerical results for a 2-dimensional advection equation with constant coefficients. We explain an algorithm of the CIP scheme applied to a 2-dimensional advection equation with variable coefficients and we show some numerical results.

Let us consider the following initial value problem of a 2-dimensional advection equation with constant coefficients;

$$\begin{aligned}\frac{\partial}{\partial t}u(t,x,y)+\begin{pmatrix}\xi_x\\ \xi_y\end{pmatrix}\cdot\nabla u(t,x,y)=0, \qquad & t>0,(x,y)\in\mathbb{R}^2,\\ u(0,x,y)=u_0(x,y), \quad & (x,y)\in\mathbb{R}^2,\end{aligned}$$

where ∇ denotes the spatial gradient $\left(\frac{\partial}{\partial x},\frac{\partial}{\partial y}\right)^T$. In the 2-dimensional CIP scheme, we need to compute not only u but also $\frac{\partial u}{\partial x}$ and $\frac{\partial u}{\partial y}$. We note that the functions $\frac{\partial u}{\partial x}$ and $\frac{\partial u}{\partial y}$ satisfy the following initial value problems;

$$\begin{aligned}\frac{\partial}{\partial t}\frac{\partial u}{\partial x}(t,x,y)+\begin{pmatrix}\xi_x\\ \xi_y\end{pmatrix}\cdot\nabla\frac{\partial u}{\partial x}(t,x,y)=0, \qquad & t>0,(x,y)\in\mathbb{R}^2,\\ \frac{\partial u}{\partial x}(0,x,y)=\frac{\partial u_0}{\partial x}(x,y), \quad & (x,y)\in\mathbb{R}^2,\\ \frac{\partial}{\partial t}\frac{\partial u}{\partial y}(t,x,y)+\begin{pmatrix}\xi_x\\ \xi_y\end{pmatrix}\cdot\nabla\frac{\partial u}{\partial y}(t,x,y)=0, \qquad & t>0,(x,y)\in\mathbb{R}^2,\\ \frac{\partial u}{\partial y}(0,x,y)=\frac{\partial u_0}{\partial y}(x,y), \quad & (x,y)\in\mathbb{R}^2.\end{aligned}$$

For discretization, let $\Delta t,\Delta x$ and Δy be positive numbers, let $Dx:=\mathrm{sign}(\xi_x)\Delta x$ and let $Dy:=\mathrm{sign}(\xi_y)\Delta y$, where "sign" means signiture function defined by

$$\mathrm{sign}(x):=\begin{cases}1 & x\geq 0\\ -1 & x<0.\end{cases}$$

Let $U^n(x,y),\partial_x U^n(x,y)$ and $\partial_y U^n(x,y)$ be approximations of $u(n\Delta t,x,y)$, $\frac{\partial u}{\partial x}(n\Delta t,x,y)$ and $\frac{\partial u}{\partial y}(n\Delta t,x,y)$ respectively. We interpolate the value $U^n(x-\xi_x\Delta t,y-\xi_y\Delta t)$ by the cubic polynomial $F(X,Y)$ satisfying

$$F(x,y)=U^n(x,y), \qquad F(x-Dx,y-Dy)=U^n(x-Dx,y-Dy),$$

$$F(x-Dx,y)=U^n(x-Dx,y), \qquad F(x,y-Dy)=U^n(x,y-Dy),$$
$$F_x(x,y)=\partial_x U^n(x,y), \qquad F_y(x,y)=\partial_y U^n(x,y),$$
$$F_x(x-Dx,y)=\partial_x U^n(x-Dx,y), \qquad F_y(x-Dx,y)=\partial_y U^n(x-Dx,y),$$
$$F_x(x,y-Dy)=\partial_x U^n(x,y-Dy), \qquad F_y(x,y-Dy)=\partial_y U^n(x,y-Dy).$$

We remark the polynomial $F(X,Y)$ is given by

$$\begin{aligned} F(X,Y) = c_{30}(X-x)^3+c_{21}(X-x)^2(Y-y)+c_{12}(X-x)(Y-y)^2+c_{03}(Y-y)^3 \\ + c_{20}(X-x)^2 + c_{11}(X-x)(Y-y) + c_{02}(Y-y)^2 \\ + \partial_x U^n(x,y)(X-x) + \partial_y U^n(x,y)(Y-y) + U^n(x,y), \end{aligned} \tag{23}$$

where

$$c_{30} = \frac{(\partial_x U^n(x-Dx,y)+\partial_x U^n(x,y))Dx - 2(U^n(x,y)-U^n(x-Dx,y))}{Dx^3}, \tag{24}$$

$$c_{20} = \frac{3(U^n(x-Dx,y)-U^n(x,y)) + (\partial_x U^n(x-Dx,y)+2\partial_x U^n(x,y))Dx}{Dx^2}, \tag{25}$$

$$c_{03} = \frac{(\partial_y U^n(x,y-Dy)+\partial_y U^n(x,y))Dy - 2(U^n(x,y)-U^n(x,y-Dy))}{Dy^3}, \tag{26}$$

$$c_{02} = \frac{3(U^n(x,y-Dy)-U^n(x,y)) + (\partial_y U^n(x,y-Dy)+2\partial_y U^n(x,y))Dy}{Dy^2}, \tag{27}$$

$$p = U^n(x,y) - U^n(x,y-Dy) - U^n(x-Dx,y) + U^n(x-Dx,y-Dy), \tag{28}$$

$$q_y = \partial_y U^n(x-Dx,y) - \partial_y U^n(x,y), \tag{29}$$

$$q_x = \partial_x U^n(x,y-Dy) - \partial_x U^n(x,y), \tag{30}$$

$$c_{12} = \frac{p+q_y Dy}{DxDy^2}, \tag{31}$$

$$c_{21} = \frac{p+q_x Dx}{DyDx^2}, \tag{32}$$

$$c_{11} = \frac{-p-q_y Dy-q_x Dx}{DxDy}. \tag{33}$$

Hence we set

$$
\begin{aligned}
U^{n+1}(x,y) &= F(x-\xi_x\Delta t, y-\xi_y\Delta t),\\
\partial_x U^{n+1}(x,y) &= F_X(x-\xi_x\Delta t, y-\xi_y\Delta t),\\
\partial_y U^{n+1}(x,y) &= F_Y(x-\xi_x\Delta t, y-\xi_y\Delta t),
\end{aligned}
$$

and we call the above scheme the 2-dimensional CIP scheme.

We show some numerical results by the 2-dimensional CIP scheme as follows. We consider the initial value problem of the 2-dimensional advection equation with constant coefficients;

$$
\frac{\partial}{\partial t}u(t,x,y) + \begin{pmatrix} -\frac{1}{4} \\ -\frac{1}{4} \end{pmatrix} \cdot \nabla u(t,x,y) = 0, \quad t>0, (x,y)\in\mathbb{R}^2,
$$

$$
u(0,x,y) = \begin{cases} 1 & \frac{1}{2} < x < \frac{3}{4}, \frac{1}{2} < y < \frac{3}{4} \\ 0 & \text{otherwise.} \end{cases}
$$

Figure 6 shows our numerical results. In these results, we take discretization parameters as $\Delta t = 1/1000$ and $\Delta x = \Delta y = 1/100$. While numerical solutions by the upwind scheme are diffused, numerical solutions by the CIP scheme coincide well with the singularity of the initial function.

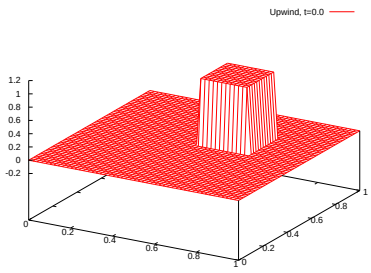

Upwind $t = 0$

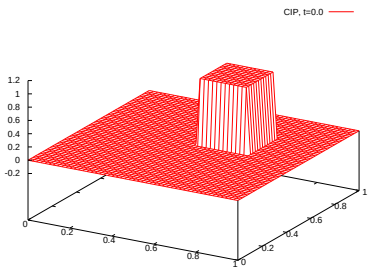

CIP $t = 0$

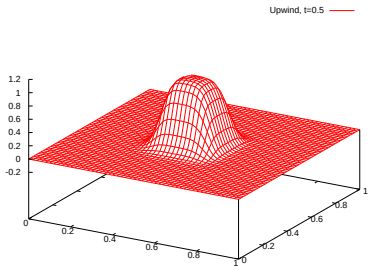

Upwind $t = 0.5$

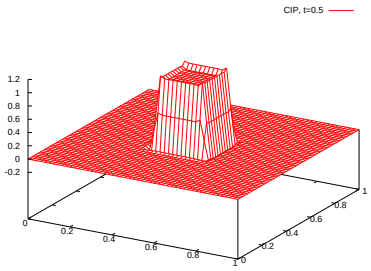

CIP $t = 0.5$

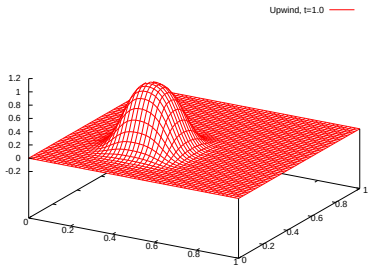

Upwind $t = 1.0$

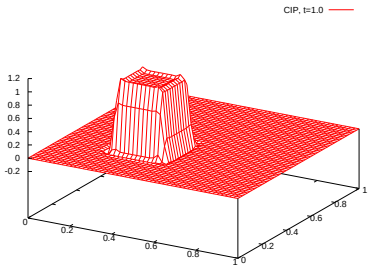

CIP $t = 1.0$

Figure 6: Numerical results for 2-dimensional advection equation with constant coefficients

Let us consider the initial value problem of a 2-dimensional advection equation with variable coefficients;

$$\frac{\partial}{\partial t}u(t,x,y) + \begin{pmatrix} -y \\ x \end{pmatrix} \cdot \nabla u(t,x,y) = 0, \qquad t > 0, (x,y) \in \mathbb{R}^2, \tag{34}$$

$$u(0,x,y) = u_0(x,y), \quad (x,y) \in \mathbb{R}^2. \tag{35}$$

The solution of the equation represents a flow of the counter-clockwise rotation around the origin with angular velocity 1. In this case, functions $\frac{\partial u}{\partial x}$ and

$\frac{\partial u}{\partial y}$ satisfy the following equations;

$$\frac{\partial}{\partial t}\frac{\partial u}{\partial x}(t,x,y) + \begin{pmatrix} -y \\ x \end{pmatrix} \cdot \nabla \frac{\partial u}{\partial x}(t,x,y) = -\frac{\partial u}{\partial y},$$
$$\frac{\partial}{\partial t}\frac{\partial u}{\partial y}(t,x,y) + \begin{pmatrix} -y \\ x \end{pmatrix} \cdot \nabla \frac{\partial u}{\partial y}(t,x,y) = \frac{\partial u}{\partial x}.$$

The equations are not homogeneous and we need the following two steps in the CIP scheme for (34)–(35): the first step is the advection phase, the latter is the non-advection phase. Algorithm 1 explains the detail of these two steps.

Algorithm 1: The CIP scheme for (34)–(35)

Initial condition:

$$U^0(x,y) = u_0(x,y)$$
$$\partial_x U^0(x,y) = \frac{\partial u_0}{\partial x}(x,y)$$
$$\partial_y U^0(x,y) = \frac{\partial u_0}{\partial y}(x,y)$$

for $n = 0$ to $\left\lfloor \frac{T}{\Delta t} \right\rfloor - 1$ **do**

Advection phase:

$$\widetilde{U}^{n+1}(x,y) = F(x - \xi_x \Delta t, y - \xi_y \Delta t),$$
$$\widetilde{\partial_x U}^{n+1}(x,y) = \frac{\partial F}{\partial X}(x - \xi_x \Delta t, y - \xi_y \Delta t),$$
$$\widetilde{\partial_y U}^{n+1}(x,y) = \frac{\partial F}{\partial Y}(x - \xi_x \Delta t, y - \xi_y \Delta t),$$

where F is given by (23)–(33).

Non-advection phase:

$$U^{n+1}(x,y) = \widetilde{U}^{n+1}(x,y),$$
$$\partial_x U^{n+1}(x,y) = \widetilde{\partial_x U}^{n+1}(x,y) - \Delta t \widetilde{\partial_y U}^{n+1}(x,y),$$
$$\partial_y U^{n+1}(x,y) = \widetilde{\partial_y U}^{n+1}(x,y) + \Delta t \widetilde{\partial_x U}^{n+1}(x,y).$$

end for

Figure 8 shows numerical results for (34)–(35) with the initial condition

$$u_0(x,y) = \begin{cases} 1 & x^2+y^2 < 1 \text{ and } y < 0.25 \text{ and } |x| < 0.2 \\ 0 & \text{otherwise,} \end{cases}$$

where Figure 7 shows the initial function. In Figure 8, we take $\Delta t = 2\pi/800$,

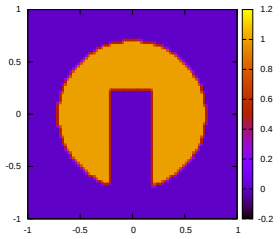

Figure 7: Initial condition $n_0(x,y)$

$\Delta x = \Delta y = 1/40$. The figures on the left side show numerical results by the upwind scheme and the those on the right side show numerical results by the CIP scheme. We note that the results by the upwind scheme are quickly diffused and are quite different from the exact solution, but we remark that numerial solutions by the CIP scheme conserve the profile of the initial condition.

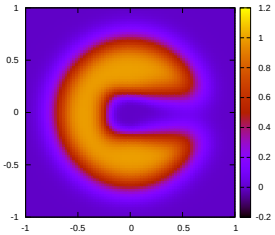

Upwind $t = \frac{1}{2}\pi$

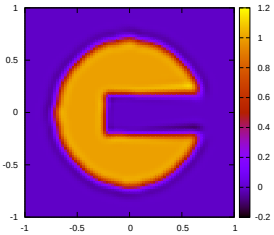

CIP $t = \frac{1}{2}\pi$

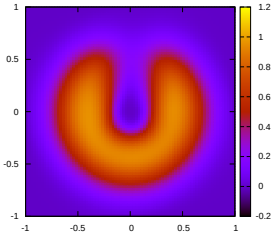

Upwind $t = \pi$

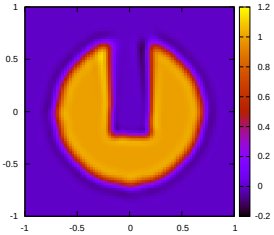

CIP $t = \pi$

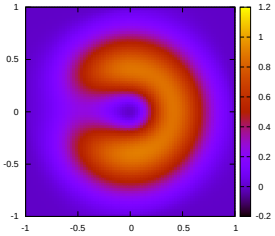

Upwind $t = \frac{3}{2}\pi$

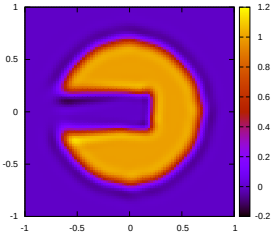

CIP $t = \frac{3}{2}\pi$

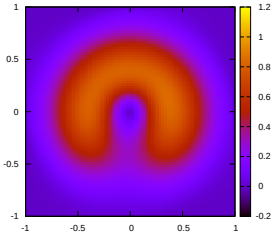

Upwind $t = 2\pi$

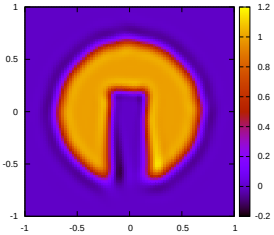

CIP $t = 2\pi$

Figure 8: Numerical results for (34)–(35)

4 Application of the CIP Scheme to the Fundamental Study of DOT

In this section, we discuss an application of the CIP scheme to the diffused optical tomography (DOT). Firstly, we slightly explain theoretical backgrounds of X-ray CT and DOT. We introduce a numerical algorithm for the transport equation using the CIP scheme, and we introduce the Radon transform with a numerical treatment of the inverse Radon transform. We show some numerical results of reconstructed attenuation coefficient, and we are sure the results imply possibility of DOT with time-resolved measurement.

4.1 Theoretical Backgrounds of X-ray CT and DOT

As we have mentioned before, light propagation in biological tissues is governed by the following transport equation;

$$\frac{\partial}{\partial t}u(t,x,\xi) + \xi \cdot \nabla_x u(t,x,\xi) + (\mu_a(x) + \mu_s(x))u(t,x,\xi) = \mu_s(x) \int_{S^{d-1}} p(\xi,\xi')u(t,x,\xi')\ d\sigma_{\xi'}. \quad (36)$$

In the equation (36), $\mu_a(x)$ is called the *absorption coefficient* and $\mu_s(x)$ is called the *scattering coefficient*. The function $\mu_t(x)$ defined by $\mu_t(x) := \mu_a(x)+\mu_s(x)$ is called the *attenuation coefficient*. The kernel function $p(\xi,\xi')$ is called the *scattering kernel* or the *phase function*. It represents probability of scattering of photon with velocity from ξ' to ξ, and it satisfies

$$p(\xi,\xi') \geq 0, \quad \int_{S^{d-1}} p(\xi,\xi')\ d\sigma_{\xi'} = 1.$$

In the study of DOT, the function defined by

$$p(\xi,\xi') := \frac{1}{2\pi}\frac{1-g^2}{(1-2g\xi\cdot\xi'+g^2)^{d/2}} \quad (37)$$

is commonly used as the scattering kernel [8] and is called the Henyey-Greenstein function [7]. In (37), the parameter g is called the *anisotropy* and describes the average of $\xi \cdot \xi'$ in a single scattering event. In biological tissues, scattering of light is highly forward scattering, and the typical value of g is considered to be 0.9 [23].

The X-ray can also be considered as a packet of photons, and it is also

governed by the transport equation. The X-rays do not scatter in biological tissues, i.e. coefficient $\mu_s(x)$ is identically zero, and the solution for the case of X-ray is expressed by

$$u(L, x_1, \xi) = u(0, x_0, \xi) \exp\left(- \int_0^L \mu_a(x_1 - s\xi)\ ds \right),$$

where $L = |\overrightarrow{x_0 x_1}|, \xi = \overrightarrow{x_0 x_1}/L$. The integral $\int_0^L \mu_a(x_1 - s\xi)\ ds$ is called the *Radon transform* of $\mu_a(x)$, and we know its inversion formula and numerical algorithm [13]. They are theoretical backgrounds of medical X-ray CT.

In the case of near-infrared light, $\mu_s(x)$ is not identically zero, and we may consider it difficult to realize DOT by a simple use of the inverse Radon transform. However, several attempts base on the idea of its use have been made to reconstruct the attenuation coefficient $\mu_t(x)$ using ovservation data of time-resolved measurement [6]. We discuss the validity of this strategy by numerical computation.

4.2 The CIP Scheme for the Transport Equation

In order to prepare scattered data for near-infrared light in biological tissues, we apply the CIP scheme to the 2-dimensional transport equation. We compute the inverse Radon transform using the forward scattered data. Our algorithm contains advection and non-advection phases the same as Algorithm 1.

Let T be a positive number. Let $\Omega := (-1, 1) \times (-1, 1)$, let $D := (0, T) \times \Omega \times S^1$ and let $\Gamma_- := \{(t, x, \xi) \in \overline{D} \mid t \in (0, T), x \in \partial\Omega, n(x) \cdot \xi < 0\}$, where $n(x)$ denotes the unit outer normal vector at x. We consider the following initial-boundary value problem for the transport equation;

$$\frac{\partial}{\partial t} u(t, x, \xi) + \xi \cdot \nabla u(t, x, \xi) + \mu_t(x) u(t, x, \xi) = \mu_s(x) \int_{S^1} p(\xi, \xi') u(t, x, \xi')\ d\sigma_{\xi'}, \quad (t, x, \xi) \in D, \quad (38)$$

$$u(0, x, \xi) = u_0(x, \xi), \quad (x, \xi) \in \Omega \times S^1, \quad (39)$$

$$u(t, x, \xi) = q(t, x, \xi), \quad (t, x, \xi) \in \Gamma_-. \quad (40)$$

For the CIP scheme, let L, M and N be positive integers and let $\Delta t =$

$T/L, \Delta x = 1/M, \Delta\varphi = 2\pi/N$. Then we generate grid points by

$$t_n := n\Delta t \ (0 \le n \le L), \quad x_{i,j} := (x_{i,j,1}, x_{i,j,2}) = (i\Delta x, j\Delta x) \ (-M \le i, j \le M),$$

$$\xi_k := (\xi_{k,1}, \xi_{k,2})^T = (\cos k\Delta\varphi, \sin k\Delta\varphi)^T \ (0 \le k \le N-1).$$

Let $U^n(x_{i,j}, \xi_k)$, $\partial_{x_1} U^n(x_{i,j}, \xi_k)$ and $\partial_{x_2} U^n(x_{i,j}, \xi_k)$ be approximations of $u(t_n, x_{i,j}, \xi_k)$, $\frac{\partial u}{\partial x_1}(t_n, x_{i,j}, \xi_k)$ and $\frac{\partial u}{\partial x_2}(t_n, x_{i,j}, \xi_k)$ respectively. We apply the composite trapezoidal rule to the integral term $\displaystyle\int_{S^1} p(\xi, \xi')u(t, x, \xi') \, d\sigma_{\xi'}$, that is, it is approximated by $\displaystyle\sum_{l=0}^{M-1} p(\xi_k, \xi_l)U^n(x_{i,j}, \xi_l)\Delta\varphi$. We compute the initial-boundary value problem (38)–(40) by the same manner as Algorithm 1: the advection term $\frac{\partial}{\partial t}u(t, x, \xi) + \xi \cdot \nabla u(t, x, \xi)$ is discretized by the CIP scheme and is computed in the advection phase, and the other terms are computed in the non-advection phase. We state the following algorithm for the initial-boudary value problem (38)–(40).

Algorithm 2: The CIP scheme for the initial-boundary value problem for the transport equation (38)–(40)

Initial condition:

$$\begin{aligned} U^0(x_{i,j}, \xi_k) &= u_0(x_{i,j}, \xi_k) \\ \partial_{x_1} U^0(x_{i,j}, \xi_k) &= \frac{\partial u_0}{\partial x_1}(x_{i,j}, \xi_k) \\ \partial_{x_2} U^0(x_{i,j}, \xi_k) &= \frac{\partial u_0}{\partial x_2}(x_{i,j}, \xi_k) \end{aligned}$$

for $n = 0$ to $N-1$ **do**
  for $i = -M$ to M, $j = -M$ to M, $k = 0$ to $N-1$ **do**
    if $x_{i,j} - \xi_k \Delta t \in \overline{\Omega}$ **then**
      Advection phase:

$$\begin{aligned} \widetilde{U}^{n+1}(x_{i,j}, \xi_k) &= F(x_{i,j,1} - \xi_{k,1}\Delta t, x_{i,j,2} - \xi_{k,2}\Delta t), \\ \widetilde{\partial_{x_1} U}^{n+1}(x_{i,j}, \xi_k) &= \frac{\partial F}{\partial X}(x_{i,j,1} - \xi_{k,1}\Delta t, x_{i,j,2} - \xi_{k,2}\Delta t), \\ \widetilde{\partial_{x_2} U}^{n+1}(x_{i,j}, \xi_k) &= \frac{\partial F}{\partial Y}(x_{i,j,1} - \xi_{k,1}\Delta t, x_{i,j,2} - \xi_{k,2}\Delta t), \end{aligned}$$

where F is given by the same manner as (23)–(33).
Non-advection phase:

$$
\begin{aligned}
U^{n+1}(x_{i,j},\xi_k) &= (1-\Delta t\mu_t(x_{i,j}))\widetilde{U}^{n+1}(x_{i,j},\xi_k) \\
&\quad + \Delta t\mu_s(x_{i,j})\sum_{l=0}^{M-1} p(\xi_k,\xi_l)\widetilde{U}^{n+1}(x_{i,j},\xi_l)\Delta\varphi, \\
\partial_{x_1}U^{n+1}(x_{i,j},\xi_k) &= (1-\Delta t\mu_t(x_{i,j}))\widetilde{\partial_{x_1}U}^{n+1}(x_{i,j},\xi_k) - \Delta t\frac{\partial\mu_t}{\partial x_1}(x_{i,j})\widetilde{U}^{n+1}(x_{i,j},\xi_k) \\
&\quad + \Delta t\mu_s(x_{i,j})\sum_{l=0}^{M-1} p(\xi_k,\xi_l)\widetilde{\partial_{x_1}U}^{n+1}(x_{i,j},\xi_l)\Delta\varphi \\
&\quad + \Delta t\frac{\partial\mu_s}{\partial x_1}(x_{i,j})\sum_{l=0}^{M-1} p(\xi_k,\xi_l)\widetilde{U}^{n+1}(x_{i,j},\xi_l)\Delta\varphi, \\
\partial_{x_2}U^{n+1}(x_{i,j},\xi_k) &= (1-\Delta t\mu_t(x_{i,j}))\widetilde{\partial_{x_2}U}^{n+1}(x_{i,j},\xi_k) - \Delta t\frac{\partial\mu_t}{\partial x_2}(x_{i,j})\widetilde{U}^{n+1}(x_{i,j},\xi_k) \\
&\quad + \Delta t\mu_s(x_{i,j})\sum_{l=0}^{M-1} p(\xi_k,\xi_l)\widetilde{\partial_{x_2}U}^{n+1}(x_{i,j},\xi_l)\Delta\varphi \\
&\quad + \Delta t\frac{\partial\mu_s}{\partial x_2}(x_{i,j})\sum_{l=0}^{M-1} p(\xi_k,\xi_l)\widetilde{U}^{n+1}(x_{i,j},\xi_l)\Delta\varphi.
\end{aligned}
$$

end if
Boundary condition:
if $(x_{i,j},\xi_k)\in\Gamma_-$ **then**

$$U^{n+1}(x_{i,j},\xi_k) = q(t_{n+1},x_{i,j},\xi_k).$$

end if
end for
end for

4.3 DOT Using Time-resolved Measurement

We use the CIP scheme to the 2-dimensional transport equation to generate scattered data and apply the inverse Radon transform to the data in order to reconstruct $\mu_t(x)$ According to Natterer [13]–[15], we introduce one of the nu-

merical methods for the inverse Radon transform, the filtered backprojection, and we compute the 2-dimensional transport equation by the CIP scheme to reconstruct the attenuation coefficient $\mu_t(x)$ by the filtered backprojection.

We start from the definition of the Radon transform.

Definition 4.1. (Radon transform)
For a function f defined on $\mathbb{R}^2$. We call the integral transform

$$Rf(\theta, x) := \int_{x\cdot\theta=s} f(x)\ d\sigma_x, \quad \theta \in S^1, s \in \mathbb{R}$$

the *Radon transform* of f, and it maps a function on $\mathbb{R}^2$ to a one on $S^1 \times \mathbb{R}$.

Let $\mathcal{S}(\mathbb{R}^2)$ and $\mathcal{S}(S^1 \times \mathbb{R})$ be the linear spaces of the rapidly discreasing functions. For $f \in \mathcal{S}(\mathbb{R}^2)$ and $g \in \mathcal{S}(S^1 \times \mathbb{R})$, we have

$$\begin{aligned}
\int_{S^1\times\mathbb{R}} Rf(\theta, s)g(\theta, s)\ dxd\sigma_\theta &= \int_{S^1}\int_{\mathbb{R}} \left(\int_{\theta^\perp} f(s\theta + z)\ dz\right) g(\theta, s)\ dsd\sigma_\theta \\
&= \int_{S^1} \left(\int_{\mathbb{R}}\int_{\theta^\perp} f(s\theta + z)g(\theta, s)\ dzds\right) d\sigma_\theta \\
&= \int_{S^1}\int_{\mathbb{R}^2} f(x)g(\theta, \theta\cdot x)\ dxd\sigma_\theta \\
&= \int_{\mathbb{R}^2} f(x) \left(\int_{S^1} g(\theta, \theta\cdot x)\ d\sigma_\theta\right) dx,
\end{aligned}$$

where $\theta^\perp$ means the orthogonal complement of θ, namely

$$\theta^\perp = \{z \in \mathbb{R}^2 \mid z\cdot\theta = 0\}.$$

The adjoint operator of R with respect to the L^2-inner product, which we denote by R^*, is given by

$$(R^*v)(x) = \int_{S^1} v(\theta, \theta\cdot x)\ d\sigma_\theta, \quad x \in \mathbb{R}^2.$$

Then we have the following theorem.

Theorem 4.1. (Natterer [13])
Let $f \in \mathcal{S}(\mathbb{R}^2)$ and let $v \in \mathcal{S}(S^1 \times \mathbb{R})$. Then we have

$$(R^*v) * f = R^*(v * Rf), \tag{41}$$

where $v * Rf$ is the convolution

$$(v * Rf)(\theta, t) = \int_{\mathbb{R}} v(\theta, t-s) Rf(\theta, s)\, ds.$$

Let us introduce the filtered backprojection method, which is one of the algorithms to compute the inverse Radon transform. The idea of the filtered backprojection is to take v such as R^*v becomes an approximation of Dirac's delta function in (41). Let ω be a positive number and suppose v_ω be the function on $S^1 \times \mathbb{R}$ defined by

$$v_\omega(\theta, s) = \frac{\omega^2}{4\pi^2} \left(\operatorname{sinc}(\omega s) - \frac{1}{2} \operatorname{sinc}\left(\frac{\omega s}{2}\right) \right),$$

where $\operatorname{sinc}(x)$ denotes the unnormalized sinc function $\operatorname{sinc}(x) = \frac{\sin x}{x}$. Then we have

$$\widehat{R^* v_\omega}(\eta) = \begin{cases} \frac{1}{2\pi} & |\eta| < \omega \\ 0 & |\eta| > \omega, \end{cases}$$

which is called the Ram-Lak filter [15]. By applying the composite trapezoidal rule to (41), we obtain the filtered backprojection algorithm for standard parallel geometry [13]–[15].

Algorithm 3: The filtered backprojection algorithm for standard parallel geometry

---

Let $\rho > 0$ and assume $\operatorname{supp}(f) \subset \{(x_1, x_2) \in \mathbb{R}^2 \mid \sqrt{x_1^2 + x_2^2} \leq \rho\}$.
Let p, q be positive intergers and let

$$\Delta\phi = \frac{\pi}{p}, \phi_j = j\Delta\phi, \theta_j = (\cos\phi_j, \sin\phi_j)^T \in S^1, \quad \text{for } p = 0, \ldots, p-1,$$

$$\Delta s = \frac{\rho}{q}, s_l = l\Delta s, \quad \text{for } l = -q, \ldots, q.$$

Data: Let values $Rf(\theta_j, s_l)$ $(j = 0, \ldots, p-1, l = q, \ldots, q)$ be given.
Step1:
for $j = 0$ to $p-1$ **do**
  for $k = -q$ to q **do**

Compute $h_{j,k}$ by

$$h_{j,k} = \Delta s \sum_{l=-q}^{q} v_\omega(s_k - s_l) Rf(\theta_j, s_l).$$

end for
end for
Step2: For each reconstruction point x, compute $f_{FB}(x)$ by

$$f_{FB}(x) = \Delta\phi \sum_{j=0}^{p-1} ((1-\vartheta)h_{j,k} + \vartheta h_{j,k+1}),$$

where $k = k(j,x)$ and $\vartheta = \vartheta(j,x)$ are determined by

$$t = \frac{x \cdot \theta_j}{\Delta s}, k = \lfloor t \rfloor, \vartheta = t - k.$$

Result: $f_{FB}(x)$ is an approximation to $f(x)$.

Finally, we compute the 2-dimensional transport equation by the CIP scheme and reconstruct the attenuation coefficient $\mu_t(x)$, from computed scattered data by use of the filtered backprojection method. Let T be a positive number larger than 2 and let $\Omega' := \{(x_1, x_2) \in \mathbb{R}^2 \mid x_1^2 + x_2^2 < 1\}$. Suppose $\mathrm{supp}(\mu_t), \mathrm{supp}(\mu_s) \subset \overline{\Omega'}$. We embed Ω' into $\Omega = (-1,1) \times (-1,1)$ and consider the initial-boundary value problem for the 2-dimensional transport equation on an extended domain Ω. For $(r,\phi) \in (-1,1) \times [0,\pi)$, we consider the following initial-boundary value problem:

$$\frac{\partial}{\partial t} u_{r,\phi}(t,x,\xi) + \xi \cdot \nabla u_{r,\phi}(t,x,\xi) + \mu_{t,\phi}(x) u_{r,\phi}(t,x,\xi) = \mu_{s,\phi}(x,y) \int_{S^1} p(\xi,\xi') u_{r,\phi}(t,x,\xi')\, d\sigma_{\xi'}, \quad (t,x,\xi) \in D, \quad (42)$$

$$u_{r,\phi}(0,x,\xi) = 0, \qquad (x,\xi) \in \Omega \times S^1, \quad (43)$$

$$u_{r,\phi}(t,x,\xi) = q_r(t,x,\xi), \quad (t,x,\xi) \in \Gamma_-, \quad (44)$$

where $\mu_{t,\phi}(x)$ and $\mu_{s,\phi}(x)$ are functions defined by

$$\mu_{t,\phi}(x) := \mu_t(x_1 \cos\phi - x_2 \sin\phi, x_1 \sin\phi + x_2 \cos\phi),$$

$$\mu_{s,\phi}(x) := \mu_s(x_1 \cos\phi - x_2 \sin\phi, x_1 \sin\phi + x_2 \cos\phi),$$

and boundary condition $q_{r,\phi}$ is given by

$$q_r(t,(x_1,x_2),\xi) := \begin{cases} 1 & x_1 = r \text{ and } x_2 = -1 \text{ and } t < 0.25 \\ 0 & \text{otherwise.} \end{cases}$$

Let $\xi^0 = \binom{0}{1} \in S^1$. Because the distance between $(r,-1)$ and $(r,1)$ equals 2, we regard $-\log\left(u_{r,\phi}(2,(r,1),\xi^0)/q_r(0,(r,-1),\xi^0)\right)$ as $R\mu_t(r,\phi)$, which is the Radon transform of $\mu_t(x)$. By application of the filtered backprojection method to the computed values, we attempt to reconstruct $\mu_t(x)$. Then we establish the following algorithm in order to reconstruce attenuation coefficient $\mu_t(x)$ from time-resolved measurement data by the inverse Radon transform.

Algorithm 4: Diffused optical tomography based on the inverse Radon transform

---

Let p, q be positive intergers and let

$$\Delta\phi = \frac{\pi}{p}, \phi_j = j\Delta\phi, \quad \text{for } p = 0, \ldots, p-1,$$

$$\Delta s = \frac{1}{q}, s_l = l\Delta s \quad \text{for } l = -q, \ldots, q.$$

Step1: Observation
for $j = 0$ to $p-1$ **do**
  for $l = -q$ to q **do**
    Observe $u_{r_l,\phi_j}(2,(r_l,1),\xi^0)$ by time-resolved measurement.
    Let $g_{j,l} := -\log\left(u_{r_l,\phi_j}(2,(r_l,1),\xi^0)\right)$.
  end for
end for
Step2: Apply the filtered backprojection method to $\{g_{j,l}\}$.
for $j = 0$ to $p-1$ **do**
  for $k = -q$ to q **do**
    Compute $h_{j,k}$ by

$$h_{j,k} = \Delta s \sum_{l=-q}^{q} v_\omega(s_k - s_l) g_{j,l}.$$

end for
end for
For each reconstruction point (x_1, x_2), compute $\mu_{t,FB}(x_1, x_2)$ by

$$\mu_{t,FB}(x, y) = \Delta\phi \sum_{j=0}^{p-1}((1-\vartheta)h_{j,k} + \vartheta h_{j,k+1}),$$

where $k = k(j, x_1, x_2)$ and $\vartheta = \vartheta(j, x_1, x_2)$ are determined by

$$t = \frac{x_1 \cos\phi_j + x_2 \sin\phi_j}{\Delta s}, k = \lfloor t \rfloor, \vartheta = t - k.$$

Result: $\mu_{t,FB}(x_1, x_2)$ is an approximation to $\mu_t(x_1, x_2)$.

We show the numerical results. In our numerical computation, we use the Henyey-Greenstein kernel

$$p(\xi, \xi') = \frac{1}{2\pi} \frac{1 - g^2}{1 - 2g\xi \cdot \xi' + g^2}$$

with $g = 0.9$ as the phase function $p(\xi, \xi')$, and the attenuation coefficient $\mu_t(x, y)$ is given by

$$\mu_t(x_1, x_2) = \begin{cases} 7 & (x_1, x_2) \in D_1 \\ 10 & (x_1, x_2) \in D_2 \\ 5 & (x_1, x_2) \in D_3 \\ 1 & (x_1, x_2) \in \Omega \backslash (D_1 \cup D_2 \cup D_3), \end{cases}$$

where

$$\begin{aligned} D_1 &:= \{(x_1, x_2) \in \Omega \mid x_1^2 + x - 2^2 < 0.25\}, \\ D_2 &:= \{(x_1, x_2) \in \Omega \mid (x_1 - 0.5)^2 + (x_2 + 0.5)^2 < 0.0625\} \backslash D_1, \\ D_3 &:= \{(x_1, x_2) \in \Omega \mid 4x_1^2 + 16(x_2 - 0.5)^2 < 1\} \backslash D_1. \end{aligned}$$

Figure 9 shows a graph of the given attenuation coefficient $\mu_t(x)$ which is a target in our inverse problem. Let $\nu \in [0, 1]$ and we assume that the scattering coefficient $\mu_s(x)$ is equal to $\nu\mu_t(x)$. We attempt to reconstruct $\mu_t(x)$ for $\nu = 0, 0.2, 0.5$ and 0.9 by Algorithm 4. In the numerical results, the discretizing parameters are $\Delta t = 1/800, \Delta x = \Delta y = 1/64, \Delta\psi = 2\pi/64$ and the parameters for the filtered backprojection are $p = 128, q = 64, \omega = 100$.

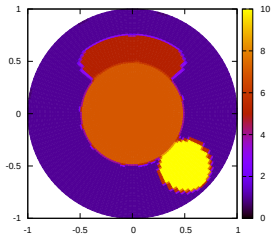

Figure 9: given attenuation coefficient $\mu_t(x)$ to be reconstructed

Figure 10 shows our the numerical results. The figures on the left side show the results by the upwind scheme and by the filtered backprojection method and the those in the right side show the results by the CIP scheme and by the filtered backprojection method. While for $\nu = 0$ the reconstructed values are close to exact values, for $\nu = 0.9$ the reconstructed image is unclear and the reconstructed values are much smaller than the exact values in both cases. For an each value of ν, however, the reconstructed values of the CIP scheme are closer to the exact values than those of the upwind scheme. We conclude that this improvement is caused by the high-accuracy of the CIP scheme. Although we can see the shape of D_1, D_2 and D_3 in the reconstructed image for $\nu = 0.9$ even by the CIP schemes, the reconstructed values are still quite different from the exact ones, and we should remark that it is still difficult to reconstruct the value of the attenuation coefficient $\mu_t(x)$ only along the strategy described above.

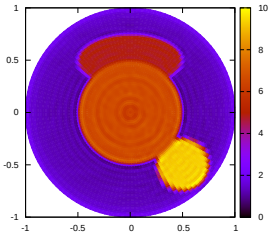

Upwind $\nu = 0$

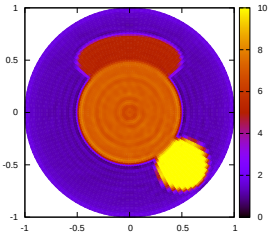

CIP $\nu = 0$

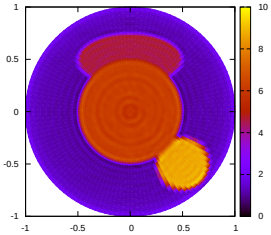

Upwind $\nu = 0.2$

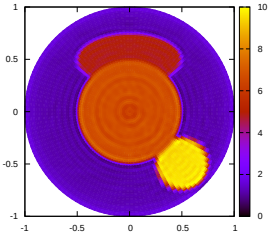

CIP $\nu = 0.2$

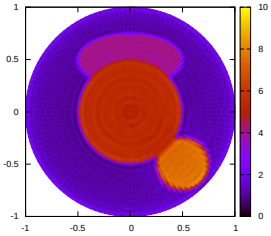

Upwind $\nu = 0.5$

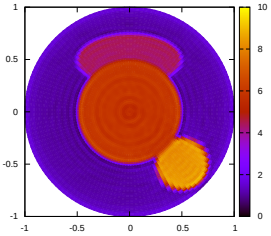

CIP $\nu = 0.5$

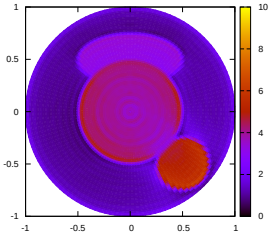

Upwind $\nu = 0.9$

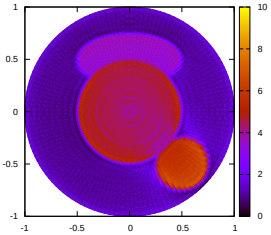

CIP $\nu = 0.9$

Figure 10: Reconstructed $\mu_t(x)$

Acknowledgments I would like to express my greatest appreciation to Prof. Iso whose enormous support and insightful comments have been invaluable during the course of my study. I would also like to thank Prof. Fukuyama, Prof. Nishida, Prof. Tomoeda and Prof. Fujiwara whose comments made enormous contribution to my work. Finally, I would like to acknowledge Prof. Matsuda and Research and Education Platform for Innovative Research on Dynamic Living Systems Based on Multi-dimensional Quantitative Imaging and Mathematical Modeling in financial support for the author's study.

References

[1] S. R. Arridge, *Optical Tomography in Medical Imaging*, Inverse Problems, **15**(1999), R41–R93.

[2] R. Courant, E. Isaacson and M. Rees, *On the Solution of Nonlinear Hyperbolic Differential Equations by Finite Differences*, Comm. Pure Appl. Math., **5**(1952), 243–256.

[3] B. Davison, Transport Theory of Neutrons, Oxford Univ. Press, London, 1956.

[4] A. Douglis, *The Solution of Multidimensional Generalized Transport Equation and Their Calculation by Difference Methods*, Numerical Solutions of Partial Differential Equations (J. H. Bramble. Ed.), Academic Press, New York, 1966.

[5] G. E. Forsythe and W. R. Wasow, Finite-difference Methods in Partial Differential Equations, John Wiley & Sons, New York, 1969.

[6] J. C. Hebden, D. J. Hall, M. Firbank and D. T. Delpy, *Time-resolved Optical Imaging of a Solid Tissue-equivalent Phantom*, Appl. Opt., **34**(1995), 8038–8047.

[7] L. G. Henyey and J. L. Greenstein, *Diffuse Radiation in the Galaxy*, AstroPhys. J., **93**(1941), 70–83.

[8] A. D. Klose, U. Netz, J. Beuthan and A. H. Hielscher, *Optical Tomography Using the Time-independent Equation of Radiative Transfer — Part 1: Forward Model*, J. Comp. Phys., **72**(2002), 691–713.

[9] H. O. Kreiss, *Über die Stabilitätsdeffnition für Differenzengleichungen die Partielle Differentialgleichungen Approximieren*, Nordisk Tidskr. Inform.-Behandling **2**(1962), 153–181.

[10] P. D. Lax and R. D. Richtmyer, *Survey of the Stability of Linear Finite Difference Equations*, Comm. Pure Appl. Math., **9**(1956), 267–293.

[11] P. D. Lax and B. Wendroff, *Systems of Conservation Laws*, Comm. Pure Appl. Math., **13**(1960), 213–237.

[12] M. Nara and R. Takaki, *Stability Analysis of the CIP Scheme* (in Japanese), Trans. Inst. Electron. Inf. Comm. Eng., Sect. A, Vol. J85-A, **9**(2002), 950–953.

[13] F. Natterer, *Numerical Methods in Tomography*, Acta Numerica, **8**(1999), 107–141.

[14] F. Natterer, The Mathematics of Computerized Tomography, SIAM, Philadelphia, 2001.

[15] F. Natterer and F. Wübbeling, Mathematical Methods in Image Reconstruction, SIAM, Philadelphia, 2001.

[16] K. Okubo and N. Takeuchi, *Analysis of an Electromagnetic Field Created by Line Current Using Constrained Interpolation Profile Method*, IEEE Trans. Antennas Propag., **55**(2007), 111–119.

[17] R. D. Richtmyer and K. W. Morton, Difference Methods for Initial-value Problems (2nd ed.), Interscience, New York, 1967.

[18] D. Tanaka, N. Higashimori and Y. Iso, *Estimates for Solutions to the Transport Equation Under the Perturbation of Its Attenuation and Scattering Terms*, Tamkang J. Math., **43**(2012), 313–320.

[19] V. Thomée, *Stability Theory for Partial Difference Operators*, SIAM Rev., **11**(1969), 152–195.

[20] K. Toda, Y. Ogata and T. Yabe, *Multi-dimensional Conservative Semi-Lagrangian Method of Characteristics CIP for the Shallow Water Equations*, J. Comp. Phys., **228**(2009), 4917–4944.

[21] S. Ukai, Transport Equation (in Japanese), Sangyo-Tosho Publishing, Tokyo, 1976.

[22] T. Utsumi, T.Kunugi and T. Aoki, *Stability and Accuracy of the Cubic Interpolated Propagation Scheme*, Comp. Phys. Comm., **101**(1997), 9–20.

[23] L. V. Wang and H. Wu, Biomedical Optics, John Wiley & Sons, New Jersey, 2007.

[24] B. Wendroff, *Well-posed Problems and Stable Difference Operators*, SIAM J. Numer. Anal., **5**(1968), 71–82.

[25] H. Takewaki, A. Nishiguchi and T. Yabe, *Cubic Interpolated Pseudo-particle Method (CIP) for Solving Hyperbolic Type Equations*, J. Comp. Phys., **61**(1985), 261–268.

[26] P. Y. Wang, T. Yabe and T. Aoki, *A General Hyperbolic Solver – the CIP Method – Applied to Curvilinear Coordinate*, J. Phys. Soc. Japan, **62**(1993), 1865–1871.

[27] F. Xiao, T. Yabe and T. Ito, *Constructing Oscillation Preventing Scheme for Advection Equation by Rational Function*, Comp. Phys. Comm., **93**(1996), 1–12.

[28] F. Xiao and T. Yabe, *Completely Conservative and Oscillationless Semi-Lagrangian Schemes for Advection Transportation*, J. Comp. Phys., **170**(2001), 498–522.